1-1-1978

Stress history study on a curved box girder.

Gerald J. Inukai

STRESS HISTORY STUDY ON A CURVED BOX GIRDER

by

Gerald J. Inukai

A Thesis

Presented to the Graduate Committee

of Lehigh University

in Candidacy for the Degree of

Master of Science

in

Civil Engineering

May 1977

This thesis is accepted and approved in partial fulfillment of the requirements for the degree of Master of Science.

May 5. 1977

Dr. B. T. Yen

Dr. D. A. VanHorn
Chairman
Department of Civil Engineering

ACKNOWLEDGMENTS

This thesis was prepared from a study being conducted at Fritz Engineering Laboratory, Lehigh University, Bethlehem, Pennsylvania. The study is sponsored by the Pennsylvania Department of Transportation and the Federal Highway Administration.

My sincere thanks to Dr. John W. Fisher, project director; Dr. J. Hartley Daniels; and especially Dr. Ben T. Yen, thesis supervisor for his assistance in organizing this thesis. The help of Mr. Hugh Sutherland and Mr. Harry Laatz is acknowledged for their help in acquiring the test data. My special thanks to Mrs. Dorothy Fielding for her invaluable aid in the preparation of this thesis.

TABLE OF CONTENTS

LIST OF TABLES

LIST OF FIGURES

LIST OF FIGURES (continued)

LIST OF FIGURES (continued)

ABSTRACT

Stress history data obtained through field testing of a curved composite box girder bridge were analyzed to evaluate the fatigue strength of the structure's details.

Details examined were the termination of transverse stiffener, the discontinuous backup bar, and the longitudinal stiffener cutoff. Strains measured at these details indicate very small equivalent constant amplitude stress ranges. These stress ranges combined with estimates on the future loadings predict the fatigue strength of the structure to be greater than that required for a service life of 30 to 40 years.

Relatively large bending stresses in the vertical direction were detected at the transverse stiffener-to-flange gap. Analysis shows that these stresses are produced when out-of-web plane forces are applied to the stiffener. Graphs are presented relating the maximum gap stresses to detail geometry and load. Connection of the stiffener to the flange at diaphragms is recommended.

The fatigue strength of the discontinuous backup bar detail is estimated to be represented by the AASHTO Category E detail. A recommendation is made to fabricate all backup bars as continuous members.

1. INTRODUCTION

A stress history investigation determines two significant variables used in evaluating the fatigue life of a structural detail, the stress range and its frequency of occurrence. These variables have been incorporated in the strength and fatigue crack growth analyses of structural details in a number of bridges[1,2,3,4]. The recorded stress range variations under vehicular loads on the bridge and the corresponding frequencies of occurrence were converted to root-mean-square (RMS) values[5], or were coupled with Miner's Hypothesis[6], to give equivalent constant amplitude stress ranges. These values were then compared with laboratory results on the fatigue strength of the details.

Stress history data are scarce for structural details of curved bridges. In an effort to obtain some field data, measurement of strain variations were taken at a number of details on a curved, composite box girder bridge under vehicular loads. The bridge is part of an approach ramp to the Fort Duquesne Bridge (I279) in Pittsburgh, Pennsylvania.

The field study also provided an opportunity to inspect the bridge details. Two of these were of interest: the termination of transverse stiffeners with attached diaphragms and the discontinuous

backup bars. The results of analyzing these two details are summarized in the report, together with the results of stress history studies.

2. DESCRIPTION OF BRIDGE AND TESTING PROCEDURE

2.1 The Bridge

The bridge under investigation is an approach ramp north of the Fort Duquesne Bridge in Pittsburgh, Pennsylvania. It carries southbound traffic onto the Fort Duquesne Bridge over the Allegheny River (Fig. 1). The bridge is anticipated to be well traveled by all types of vehicles including heavily loaded trucks from the northern portions of Pittsburgh.

The approach ramp consists of a number of three-span, continuous, curved bridges. The portion under investigation has two concentric rectangular steel box girders with a composite reinforced concrete deck (Fig. 2). Each span has a centerline arc length of 30.5 m (100 ft.). The radius of curvature for each span is constant but varies between spans, being 260 m (853 ft.), 263 m (863 ft.), and 260 m (853 ft.), respectively. The bridge is supported on radial steel bents. The test span was the middle span, between Bents SB11 and SB12.

The cross-sectional dimensions of the box girders vary along the length of each span. A cross section at an interior diaphragm is shown in Fig. 3. Interior diaphragms are spaced at 3.048 m (10 ft.) intervals. The box girders contain typical transverse and longitudinal stiffeners.

2.2 Instrumentation

Forty-eight electrical resistance strain gages of foil type were mounted at various details and at a few nominal cross sections of the box girders (as shown in Fig. 4). The details under investigation included the transverse and longitudinal stiffeners and the backup bars at longitudinal butt welds.

Out-of-plane forces exerted from diaphragm members onto the transverse stiffeners may cause large plate-bending stresses in the web between the end of the stiffeners and the flange. Strain gages were placed around this area. The bottom flange longitudinal stiffeners in the test span extend throughout the bridge with some terminating in the positive moment region, 9.1 m (30 ft.) from the interior support bents. Strain gages were applied on the bottom flange at the end of a number of these stiffeners.

The backup bars are small rectangular steel bars tack-welded at the bottom flange-to-web connections along the length of the box girder. The bars were placed inside the box girder to aid fabrication and were left in place in the bridge, thus becoming an integral part of the bridge box girder. The small gap between two adjoining steel bars constitutes a discontinuity for stress flow hence is a structural detail potentially weak in fatigue strength. Strains in the flange at some of these gaps were monitored.

Cross sections where strain gages were installed for stress evaluation were at one end, at a quarter point, and at the middle of the test span (Fig. 4). All strain gages were connected to

analog trace recorders which depict strain variations on oscillographs. Some tracings of oscillographs are shown in Fig. 5 as examples. From these graphs, stress ranges and frequencies could be determined.

2.3 Field Testing

The field testing of the bridge included a control load test and the stress history acquisition. During the control load test, the Federal Highway Administration's test truck traveled across the test span in each of the three lanes (Fig. 2) at two speeds, 8 km/h (5 mph) and 80 km/h (50 mph). The test truck simulated the standard HS20 loading (Fig. 6). During the test truck runs, the bridge was cleared of all traffic. Table 1 summarizes the test truck run conditions.

The test truck crawl runs (8 km/h)(5 mph) simulated a static load condition, load without impact. Data obtained from this portion of the test were used for comparing with computed results. Data from the speed runs (80 km/h)(50 mph) were used in the comparison of static and dynamic responses of the bridge.

The stress histories of the strain-gaged details were compiled over five continuous days of measurement, giving a representative sample of stress variations due to different vehicles. When trucks, semi-trailers and buses capable of producing stress fluctuations were approaching, the trace recorders were started

simultaneously. The resulting oscillographs were labeled with the vehicle type according to the standard FHWA truck classification (Fig. 7). Each vehicle produced a set of traces which were to be measured for stress ranges. A stress range was the difference between the maximum and minimum stress for each trace.

3. TEST RESULTS

3.1 Controlled Load Test

The two groups of controlled load tests conducted on the bridge were the crawl run (static) and the speed run (dynamic).

Oscillograph traces for the crawl runs were measured for strains as a function of the truck's position on the bridge. The strains can be converted to stresses resulting in a plot analagous to the influence line for a given gage location. An example is given in Fig. 8 comparing the oscillograph trace of a longitudinal flange gage to the influence line of bottom flange stress at midspan of a three-span continuous beam.

Stresses measured at a given truck location can be used to determine the accuracy of the stresses computed through the finite element analysis of the bridge. A finite element analysis of the structure was made using the program SAP IV[7]. In simplifying the problem, the bridge was assumed prismatic in cross-sectional dimensions with nominal wall thicknesses described by the design drawings. Symmetry about midspan was used to reduce the model size. The concentric boxes were assumed to act independent of each other when the load was applied over one box. The inner box was chosen for discretization. These assumptions reduced the model to a quarter

discretization, Fig. 2. The model was discretized into plane stress and plate bending elements for the flanges and webs, beam elements for the stiffeners and truss elements for the diaphragms. Stress at various details could be determined by substructuring.

A comparison of longitudinal web stresses at midspan was made between the measurements from oscillograph traces and the values from the finite element model, Fig. 9. Two concentrated loads placed over the webs at midspan simulated the test truck. Their total was equal to the test truck gross weight of 298 kN (67 kips) distributed to the webs for a lane 1 loading. The results in Fig. 9 indicate the model is an adequate representation of the actual structure. Generally the measured values were lower than the computed values due to the loading assumption of concentrated loads versus actual axle distribution.

The speed runs were used in the determination of dynamic effects on the stresses in the structure. The oscillograph trace from a static (crawl) run and that from a dynamic (speed) run are compared in Fig. 10 for a point on the bridge. It can be seen that the curves are identical in overall shape. The speed run contained dynamic strains which were superimposed on the static strain curve. The dynamic strains had a higher frequency than the static strain but were smaller in magnitude. The difference between the dynamic and static curves reveals the dynamic effects of the truck on the

stress and strain at the point of the gage and is an indication of the impact factor for the bridge.

The lateral position of a truck influences the stress at a point of a multi-lane bridge. Three oscillograph traces for a point on the bottom flange of the inner box girder are compared in Fig. 11, each for a different lateral position of the test truck on the bridge. The stresses were highest when the truck was directly over the box girder (Lane 1). The stress magnitudes decreased when the vehicle was further away from the gage (Lanes 2 and 3). When the test truck was in Lane 3, the furthest from the gage, the stress magnitude remained 24 percent of the maximum Lane 1 stress. This is an indication of the load distribution characteristic of the box girder bridge, and implies that trucks in all lanes of the bridge must be considered in evaluating the stress history of bridge details.

3.2 Stress History

Oscillograph recordings were made for all large vehicles crossing the test span during a five day period. Small vehicles such as cars and pickup trucks produced negligible stress ranges in the bridge and were not recorded. Details which sustained only very low stresses during the control load test were excluded from further measurements. Each of the significant oscillograph traces were measured for stress range under the assumption of one stress range per vehicle passage[2]. The stress ranges were grouped according

to magnitude and were plotted as stress range histograms. The histogram for the bottom flange at longitudinal stiffener cutoff is shown in Fig. 12. Histograms were prepared for each gage and are presented in the Appendix.

From reviewing the stress range histograms, it can be found that the frequency of higher stress ranges was relatively low for most of the bridge details. One of the factors contributing to this condition was the distribution of traffic volume. During the five days of stress history recording, a total of 1424 trucks travelled on this section of the bridge. Lane 1 is at the end of an entrance lane with a small divider separating it from the other two lanes, thus only carrying on-coming trucks. About one-third (34.3 percent) of the total truck traffic came on the bridge from here. Lanes 2 and 3 contained the major flow, with 52.5 percent in the curb lane and 13.2 percent in the passing lane, Lane 3. Since Lane 2 is between the two box girders, loads in this lane were distributed to both box girders resulting in lower stress magnitudes. Hence only a small percent of the traffic generated large strain ranges in the box girders. Further discussion on this will be made later in Chapter 6.

4. TERMINATION OF TRANSVERSE STIFFENER DETAIL

One of the structural details which incurred relatively high stress ranges was the termination of transverse stiffeners. The most serious of these details occurred when the transverse stiffeners were part of an internal diaphragm in the box girders. The vertical bending stress at the gap between the flange and the end of the stiffener had a maximum value of 31.7 MN/m^2 (4.6 ksi).

Both AISC[8] and AASHO[9] design specifications permit the termination of the transverse stiffeners short of the tension flange at all intermediate locations (Fig. 13). When a transverse stiffener is part of an interior diaphragm, forces may be introduced to the stiffener, moving it out of the plane of the web. Stiffeners not connected to the flange will displace relative to the flange. This relative displacement concentrates in the area between the stiffener and flange, producing large bending stresses on the web surfaces.

All intermediate transverse stiffeners in the Fort Duquesne approach spans are terminated short of the tension flange. Some of these stiffeners serve as a part of the interior diaphragms. Strain gages at one of these stiffener ends recorded the high stresses as reported above.

Stresses at the gap were computed from the substructuring of the overall finite element model. Two finite element models were employed for this study. The first was a replica of the detail in the test span. This substructure contained node points which corresponded to nodes on the overall bridge analysis model. Nodal displacements and rotations in the overall analysis were used as loads on the substructure. Results from the substructure are given in Table 3 with a comparison to the field test results. A good correlation exists between the two groups of stresses. From this outcome, it can be assumed that the substructure model accurately describes the behavior of the actual structural detail. The maximum computed stress in the substructure's stiffener gap was 159 MN/m^2 (23 ksi) when the bridge is subjected to a HS20 load at midspan of the center span.

To explore further the magnitudes of the out-of-plane bending stresses at the transverse stiffener gap, a parameter study was made using a finite element model similar to that used for the box girder detail substructuring (Fig. 13). The variables that were studied were the thickness of the flange, the thickness of the web, and the stiffener to flange gap length. Model boundary conditions were assumed hinged providing least restraint to the model. A concentrated load was placed on the stiffener to simulate the effect produced by a diaphragm. The stresses then obtained would be an upper bound value due to the under estimation of actual restraint at model boundaries and the disregard of stress relaxation of the diaphragm.

The results of a 9 mm (3/8 in.) web subjected to a unit load are shown in Fig. 14. The out-of-plane bending stresses increase with the length of the gap until it reaches a maximum. For a given gap length, the maximum stress occurs at the top or the bottom of the gap, depending on the thickness of the flange.

For an identical model subjected to a unit lateral displacement (instead of a unit load) at the transverse stiffener, the stresses at the gap decrease with increasing gap length, as is shown in Fig. 15. In other words, a larger gap would be preferable to a smaller one with regard to lateral displacement.

In box girder design and analysis, whether force or displacement is computed is a matter of analytical procedure. By using force as the controlling unit, various combinations of the parameters were investigated in this study. The results show a linear relationship between the logarithm of bending stresses and the logarithm of web thickness for any gap length to web thickness ratio. This relationship is depicted in Figs. 16 to 23.

In algebraic form, the relationship is

$$\frac{\sigma_g}{P} = C\, t_w^{-k} \qquad (1)$$

where

σ_g = bending stress at top or bottom of gap

P = diaphragm force

C = constant for a given flange-to-web thickness ratio

k = exponential constant for top or bottom of gap

This equation is valid for conventional transverse stiffeners which are cut short from the flange and are a part of an interior diaphragm in a rectangular box girder.

Figures 16 to 23 indicate large stresses will be produced in thin webs if lateral force is introduced at a transverse stiffener gap. Large stresses due to live loads may cause fatigue cracks to occur at the gap.

For given box girder component dimensions, the large stress may be reduced by decreasing the gap length. A positive solution to the problem would be the elimination of the relative displacement between the stiffener and the flange. This could be achieved by welding the transverse stiffener to the flange.

5. DISCONTINUOUS BACKUP BAR

The backup bar is a fabrication aid used to facilitate the welding of two plates. It is usually tack welded to the back of the joint to contain molten weld metal. The backup bars in the test span were used at the bottom flange-to-web plate joints (Fig. 24). Each of the bars is rectangular in cross section (6 x 19 mm). They were tack welded to the inside of the joint and the groove weld was made from the outside. The backup bars run the full length of the three span box girders.

The AWS Structural Welding Code[10] states that all backing strips must be made continuous. In practice, sometimes backup bars are placed butted against each other without welding. This procedure results in a continuous strip to contain the molten weld metal but discontinuities remain in the backup bar itself. When the discontinuities are oriented perpendicular to the stress field, consideration must be given to fatigue crack propagation.

The backup bar discontinuities in the test span are oriented perpendicular to the longitudinal bending stress field. By compatability, the backup bar experiences the same high magnitude of strain and stress as the web-to-flange joint.

To examine the fatigue strength of the discontinuous backup bar detail, subcritical crack growth is considered. The crack growth equation[11] is rearranged as

$$dN = \frac{da}{C \Delta k^n} \tag{2}$$

where a = crack size

N = life, in cycles

C & n = material constants

Δk = change in stress intensity

The change in stress intensity factor may be computed using the expression[12]

$$\Delta k = F_e F_w F_s F_g \Delta \sigma \sqrt{\pi a} \tag{3}$$

where $F_e = 2/\pi$, for penny-shaped cracks

$F_w = \sqrt{\sec(\pi a/2t)}$, for finite width plate[13]

$F_s = 1.12$, for surface crack[13]

F_g = correction factor for stress concentration at the detail, a function of the crack size

$\Delta \sigma$ = applied normal stress range at the detail

A finite element analysis of the discontinuous backup bar detail was completed to determine the stress concentration[14]. From the results, a stress concentration decay curve was determined in terms of the crack size "a", as shown in Fig. 25. A polynomial

equation for the stress concentration correction factor was derived from this decay curve[12].

By using the values of the correction factors F_e, F_w, F_s, and F_g, Eq. 2 is then in terms of N, $\Delta\sigma$, and a. Integration from the initial flaw size to the tolerable flaw size results in an estimate of the fatigue life of the detail. The initial flaw size was assumed 0.762 mm (0.03 in.). The tolerable crack size was taken as the effective thickness of the material (Fig. 24). The result of the integration is a relation between stress range and life as given in Fig. 26. The relationship is very close to the AASHTO fatigue category E[15] detail. This implies that care must be taken to control the stress at the backup bar discontinuity or alternately, such discontinuities must be avoided.

A refined analysis needs to be conducted to assess more accurately the fatigue strength of the discontinuous backup bar detail. An evaluation of the backup bar fatigue strength is given in the next chapter.

6. CUMULATIVE DAMAGE

Magnitudes of stress ranges were low at most of the gage locations on the Fort Duquesne Bridge approach test span. The maximum recorded stress range of most gages, as shown in the stress range histograms (Appendix A) are far below the corresponding permissible stress range of AASHTO[15]. Therefore, it is not likely that any fatigue failure will occur in this test span.

The highest stress range value from measurements was from the vertical bending gage near the transverse stiffener cutoff. Its value was 43 MN/m^2 (6.23 ksi). The stress in the gap is probably higher. Comparison to the results of the finite element substructure shows the stress in the gap to be 3.5 times greater than the stress at the vertical gage location. Caution must be exercised when using the measured results.

Because of the uncertainty in the long term, high cycle fatigue behavior of structure details, the cumulative effects of stress ranges at a number of details were examined, ignoring the "thresholds" of the fatigue strength categories. The stress range histograms of these gages were converted to root-mean-square (RMS) stress ranges[5] and are listed in Table 2. These equivalent constant amplitude stress ranges intercept the extended fatigue strength

lines at very high number of cycles, indicating long life. If Miner's hypothesis[6] is used with the fatigue strength lines, similar results are obtained. Figure 27 summarizes some of these comparisons.

The number of trucks monitored during the test period of 84 hours was 1424, giving an average daily truck traffic (ADTT) of 407. By assuming a high annual increase rate of 3 percent, the total truck volume in 40 years is 11.54 million. This is more than an order of magnitude lower than the value which might cause fatigue damage.

If the RMS gross vehicle weight of trucks increases 30 percent in the future due to reasons such as the development of industrial plants or increase of traffic directly over the box girders, the RMS stress ranges or the equivalent stress ranges incorporating the Miner's hypothesis can be conservatively increased by 30 percent. The resulting life of possible fatigue damage is still an order of magnitude higher than the traffic volume (Fig. 27). Cumulative damage due to fatigue thus does not appear to be a matter of concern.

7. CONCLUSION AND RECOMMENDATIONS

The field test and subsequent data reduction and analysis of the Fort Duquesne approach spans has resulted in the following conclusions:

1. The test span was over-designed for fatigue.
2. Intermediate transverse stiffeners when part of internal diaphragms and cut short of the flange generate large, possibly hazardous bending stresses in the web.
3. Discontinuous backup bar details are an AASHTO Category E detail.

The over-design of the test span may have resulted from simplified analysis methods leading to conservative design. Using a finite element model, more accurate estimates of stresses can be made and a more economical design may be produced.

Stress history measurements on the test span indicate small equivalent constant amplitude stress ranges for the details. In each case, the equivalent stress range value was below the fatigue threshold level of all categories of details. Since some of the actual stress range values were greater than the threshold value, fatigue cracks will propagate. A conservative approach was taken when the inclined portion of the S-N curve was extended to account for the

smaller stress ranges. Values of fatigue life, estimated using this assumption indicate a full useful service life of the bridge.

Out-of-plane forces produced by internal diaphragms can induce large bending stresses in the web at the end of the transverse stiffener. These large stresses, resulting from the relative displacement of the flange and stiffener, can become a fatigue problem. A simple solution would be to extend the stiffener and weld it to the flange. This would eliminate the relative displacement. Care must be taken to avoid another fatigue problem caused by the weld. Longitudinally, the weld would be an AASHTO Category C detail, under the structure bending stress. This produces no new problems since the stiffener to web connection is the same type of detail under the same stress. Transversely, the stiffener to flange connection is an AASHTO Category E detail. The class of detail has become worse but the detail is subjected to a much lower stress range.

The discontinuous backup bar fatigue problem can be eliminated if the bars are made continuous as recommended by AWS. If the discontinuity is removed, no stress raiser will exist, thus eliminating the problem.

High cycle fatigue problems at welded bridge details can be reduced if these design recommendations are followed.

TABLE 1 SUMMARY OF CONTROL TRUCK RUNS

Run	Lane	Speed
1	3	Crawl
2	2	Crawl
3	1	Crawl
4	1	72 km/hr
5	2	80 km/hr
6	3	77 km/hr
7	2	72 km/hr
8	1	69 km/hr
9	3	77 km/hr

TABLE 2 EQUIVALENT CONSTANT AMPLITUDE STRESS RANGES

FOR GAGE LOCATIONS

Gage	$S_{r\ rms}$ (MN/m^2)	$S_{r\ Miner}$ (MN/m^2)	Location
5	7.12	8.40	IB, END, BF
8	4.01	4.67	IB, BB
11	8.12	9.52	IB, LS
12	8.48	10.08	IB, LS
13	5.36	6.53	IB, 1/4, BF
19	8.89	10.20	IB, MID, BF
21	7.12	8.40	IB, MID, BF
26	6.65	7.64	IB, TS, H
27	11.65	13.34	IB, TS, V
31	7.18	8.50	IB, BB
46	7.65	8.62	OB, MID, BF
50	6.53	7.33	OB, BB

IB	Inner box	LS	Longitudinal Stiffener
OB	Outer box	TS	Transverse stiffener
END	End of span	H	Horizontal gage
1/4	Quarter span	V	Vertical gage
MID	Midspan		
BF	Bottom flange		
BB	Backup bar		

TABLE 3 COMPARISON OF COMPUTED AND MEASURED STRESSES IN TRANSVERSE STIFFENER GAP

	Computed (MN/m^2)	Measured (MN/m^2)
Vertical Gage	- 43	- 32
Horizontal Gage	9.3	8.3
Maximum Gap Stress	165	---

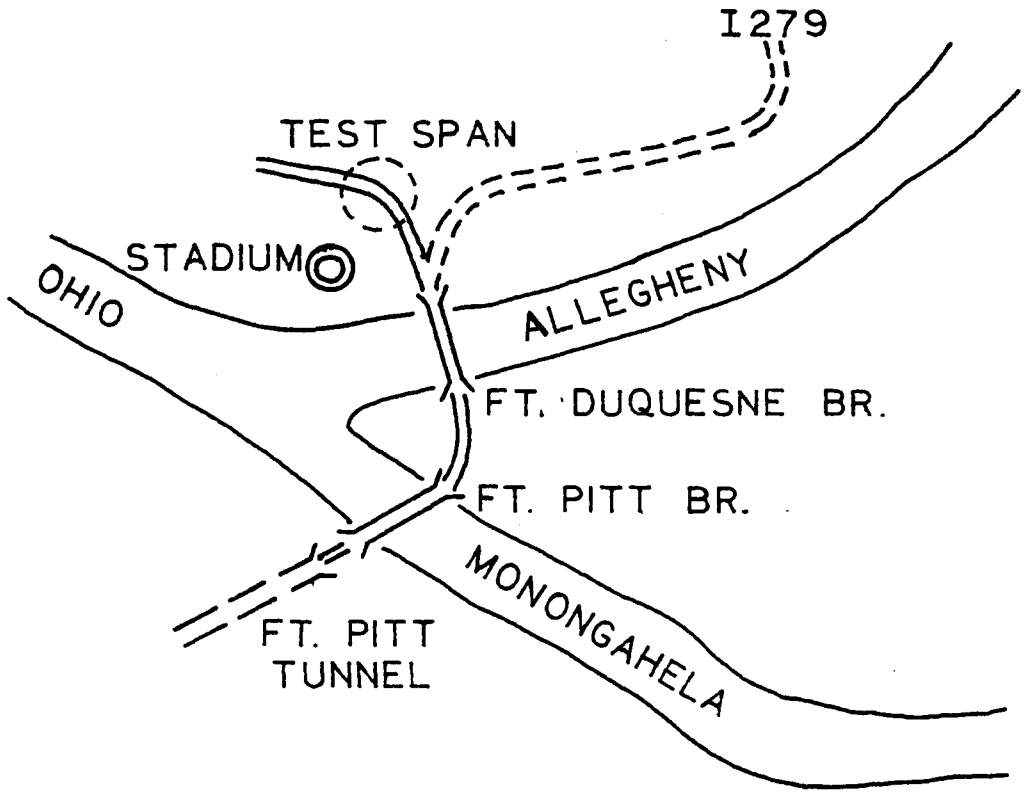

Fig. 1 Test Site

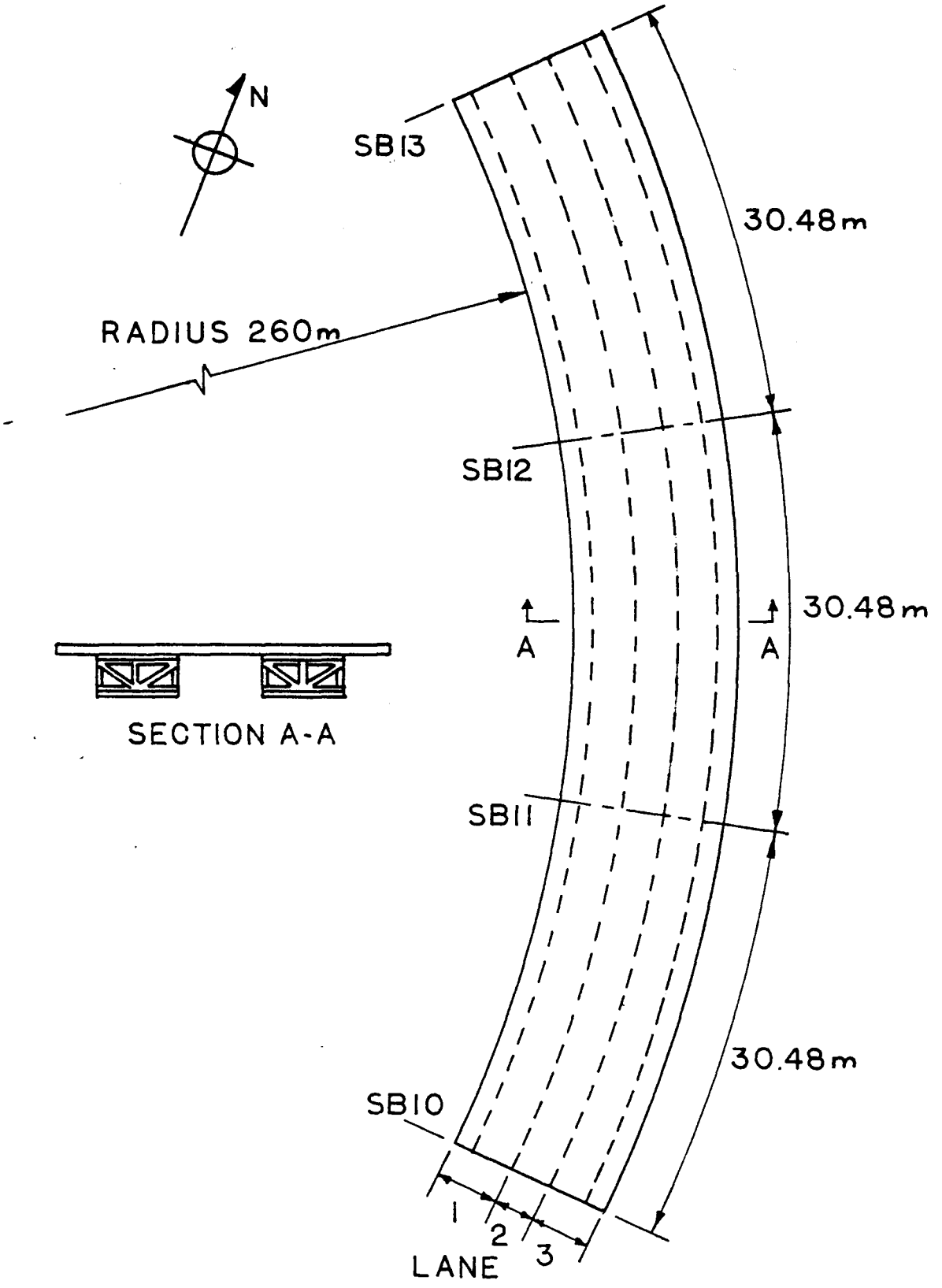

Fig. 2 Test Span

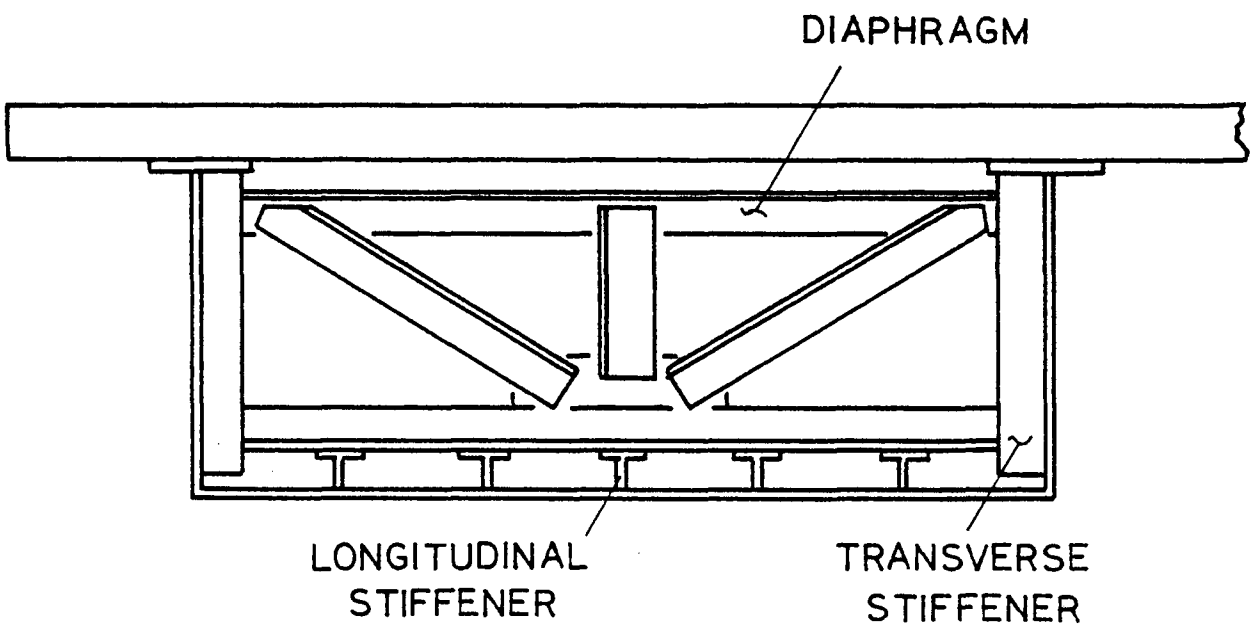

Fig. 3 Typical Cross Section Showing

One Box and Details

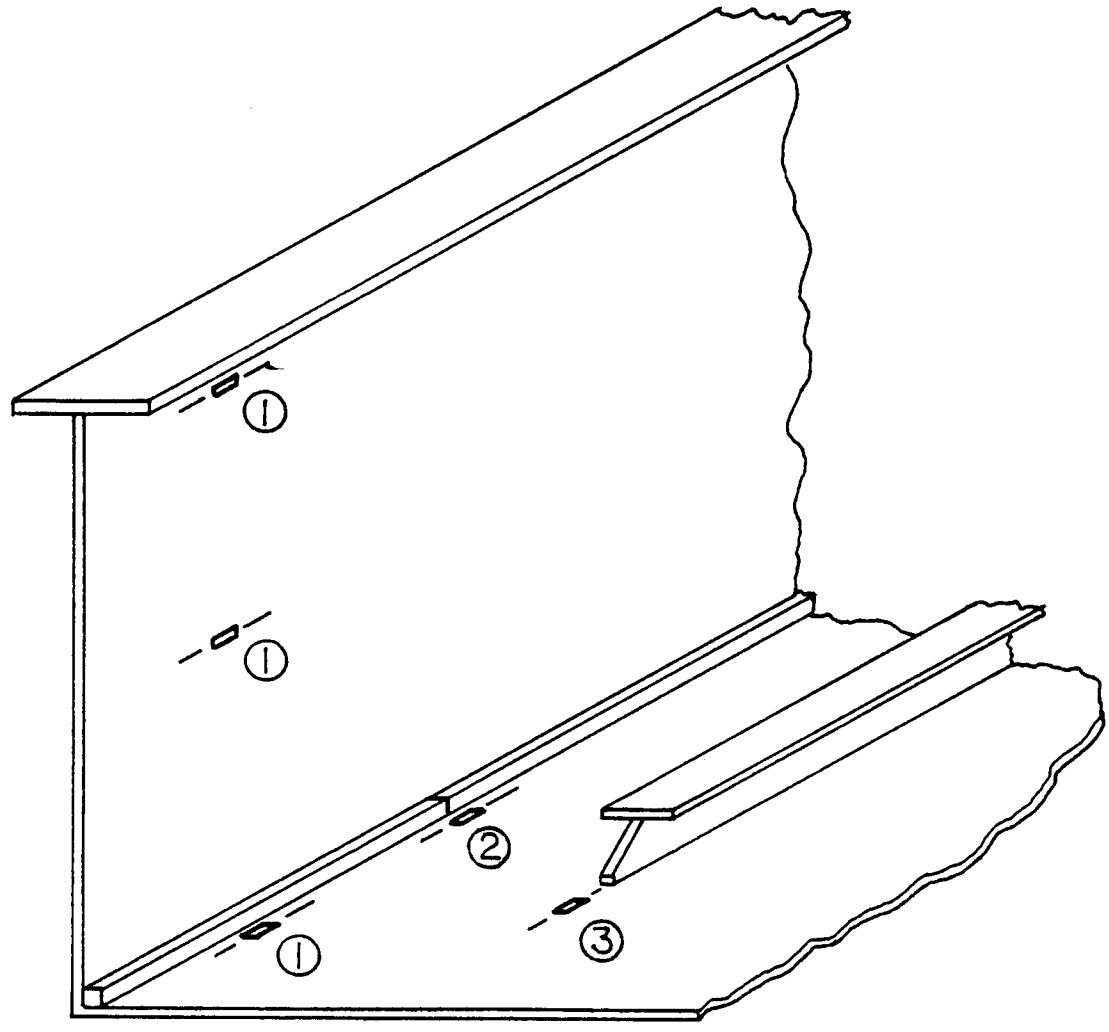

① BENDING STRESS

② BACKUP BAR

③ LONGITUDINAL STIFFENER

Fig. 4a Strain Gage Locations

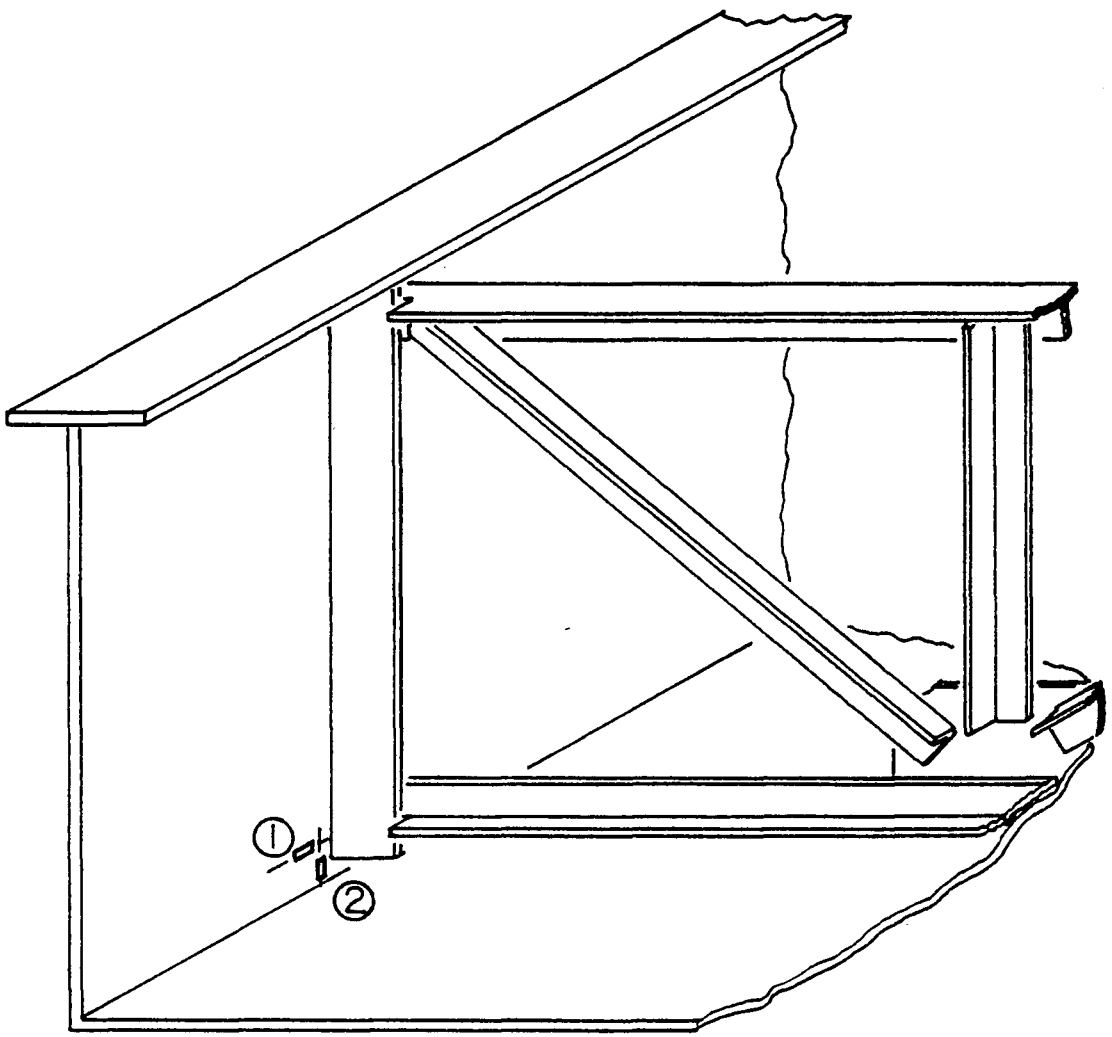

① TRANSVERSE STIFFENER HORIZONTAL GAGE

② TRANSVERSE STIFFENER VERTICAL GAGE

Fig. 4b. Strain Gage Locations

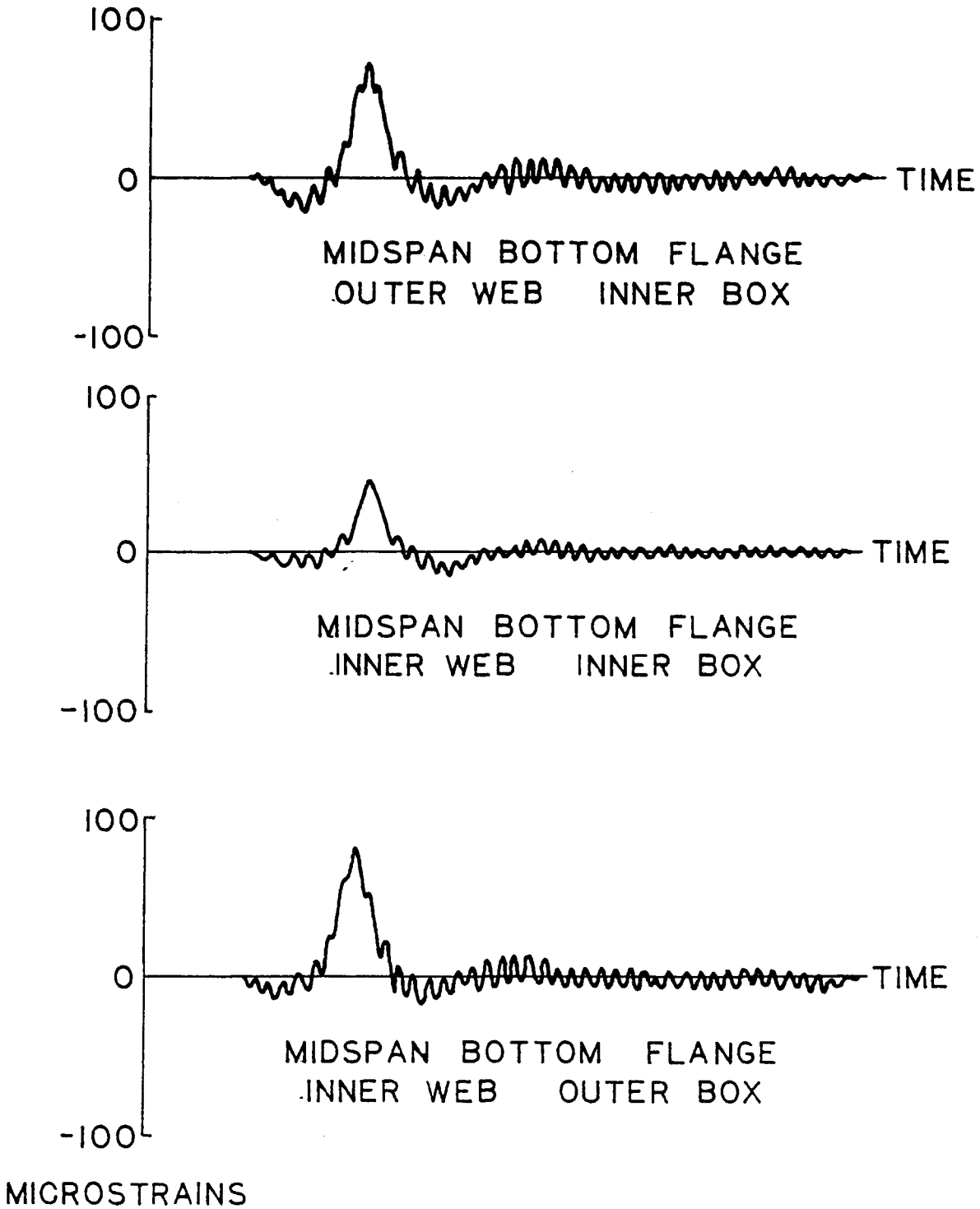

Fig. 5 Oscillograph Traces

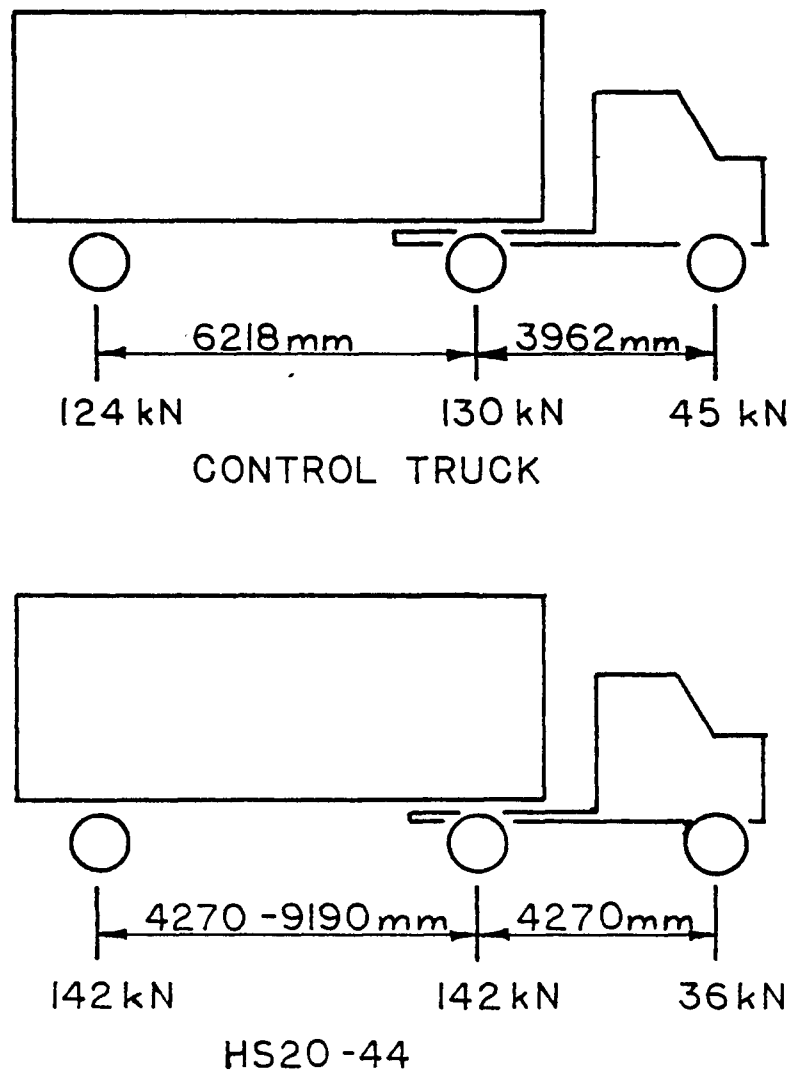

Fig. 6 Comparison of Control Truck to HS20-44

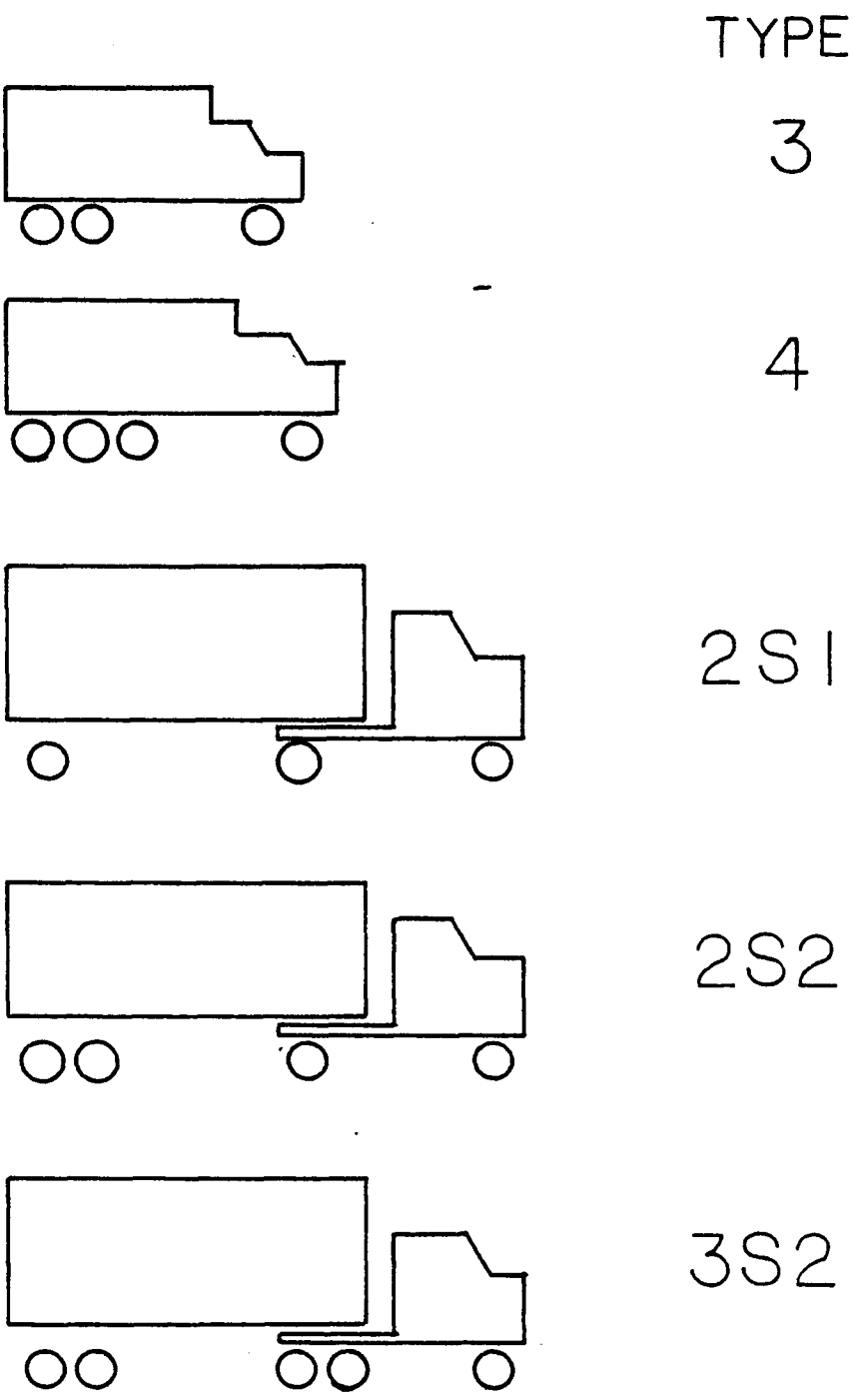

Fig. 7 FHWA Truck Classification

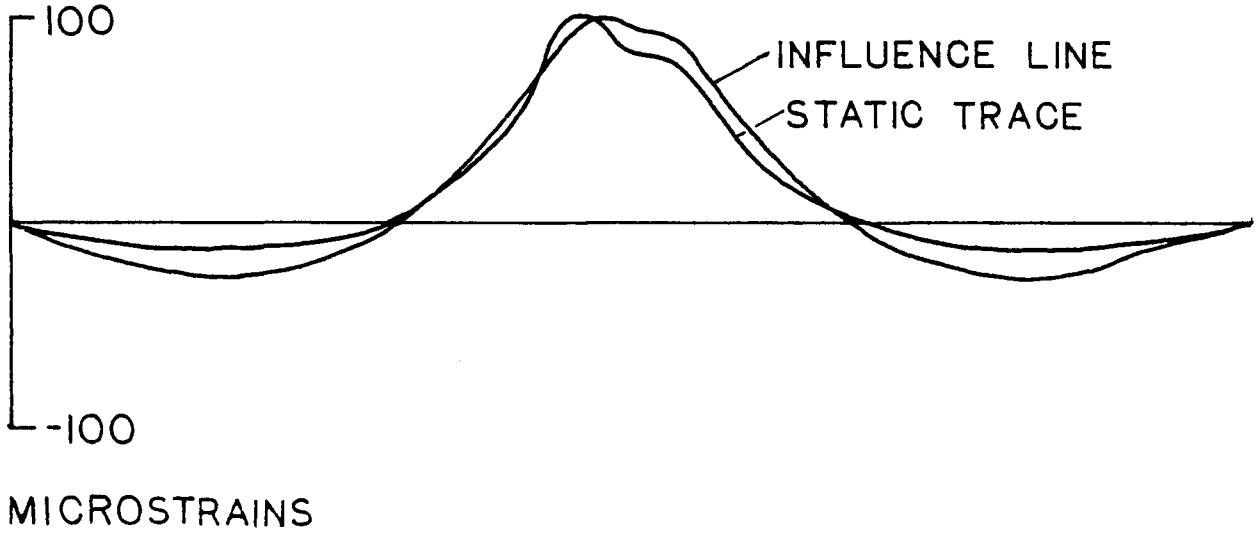

Fig. 8 Comparison of Influence Line and Static Run Oscillograph Trace

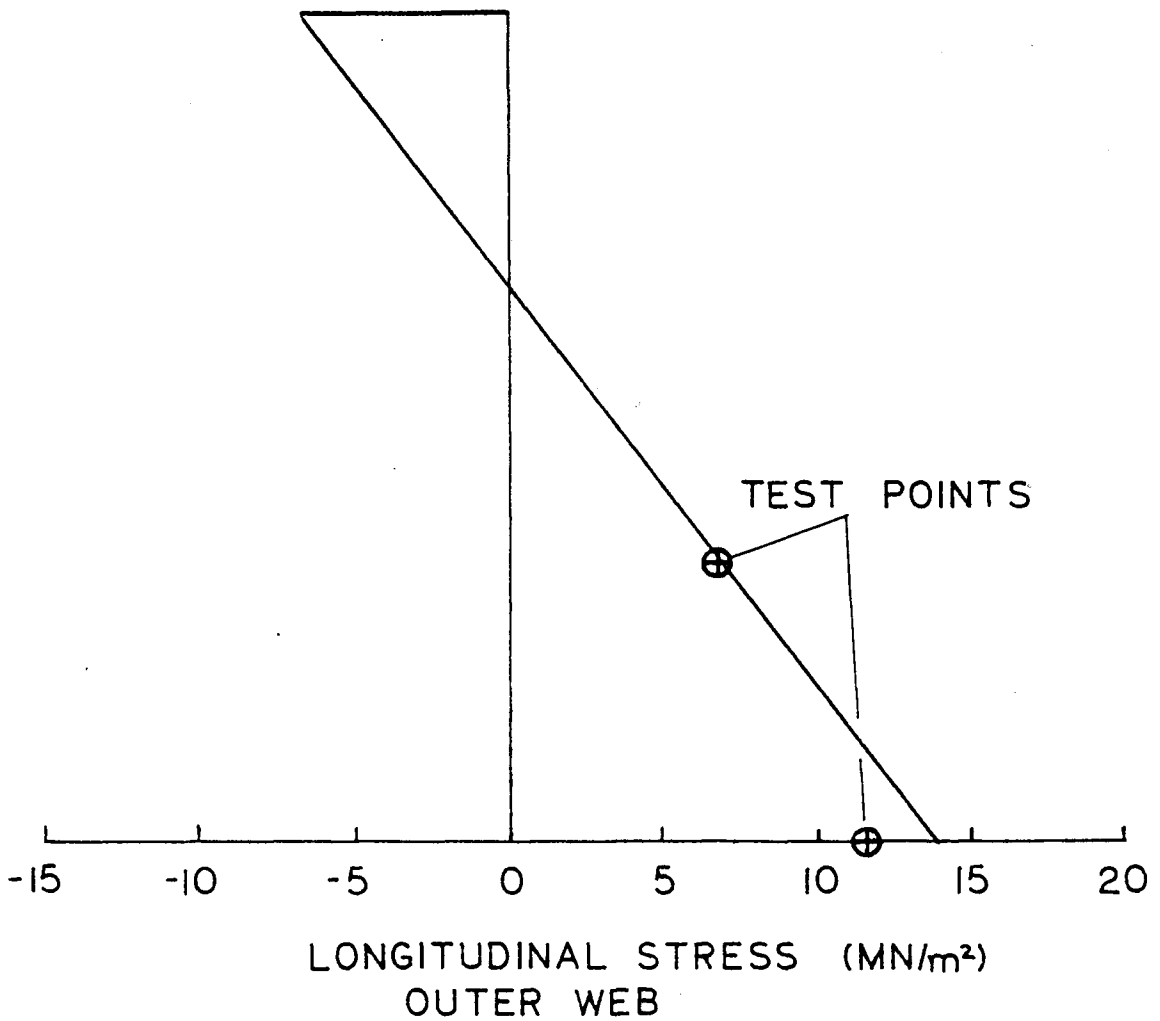

Fig. 9 Comparison of Finite Element Model Results to Measured Test Results

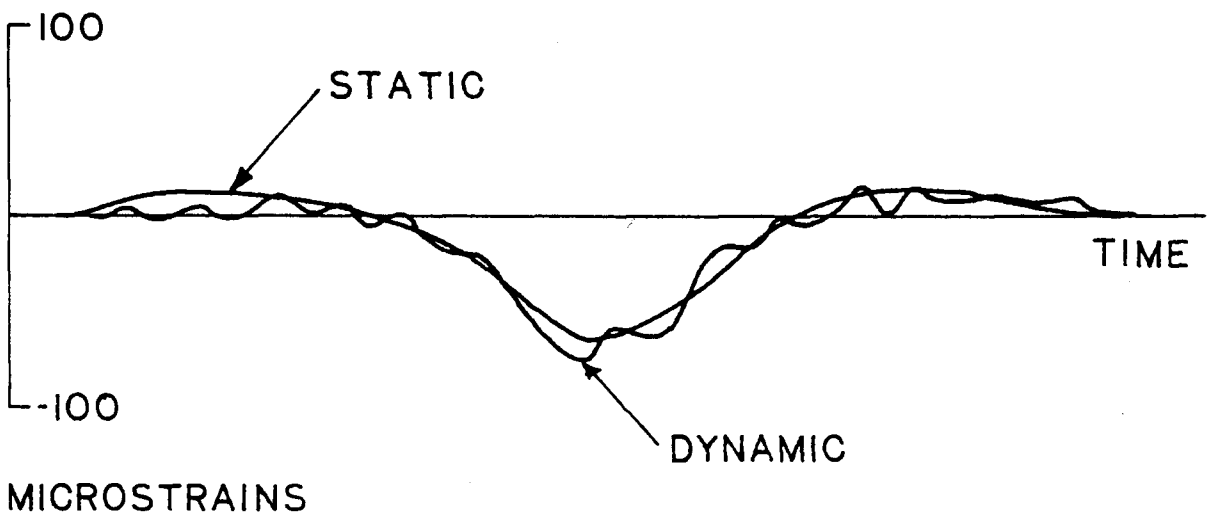

Fig. 10 Comparison of Static and Dynamic Oscillograph Traces

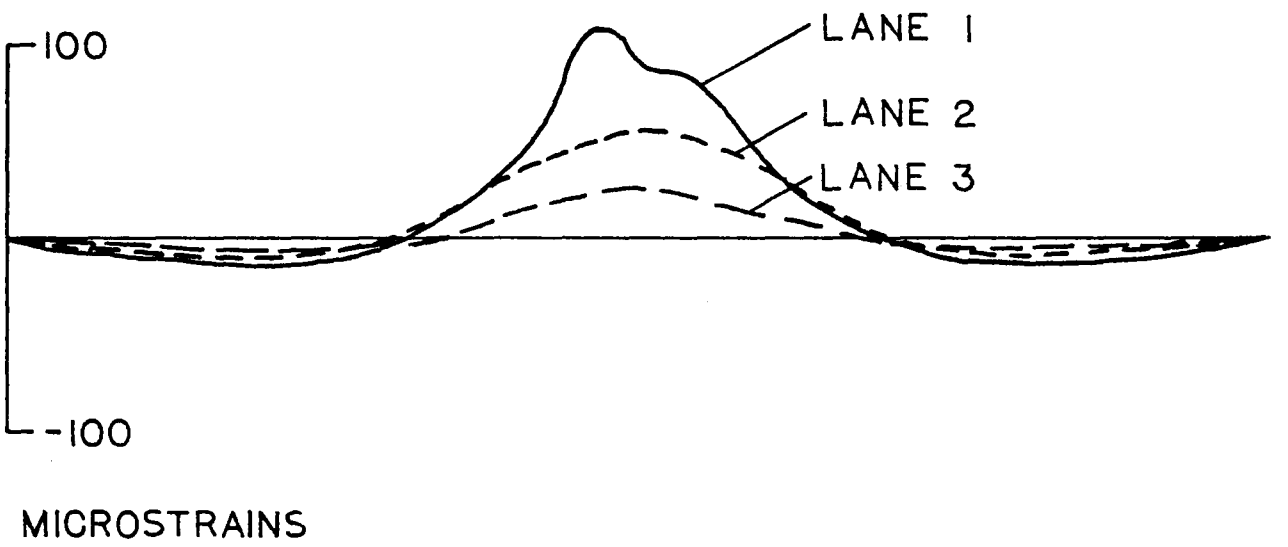

Fig. 11 Effect of Lateral Position of Load on Bottom Flange Stress

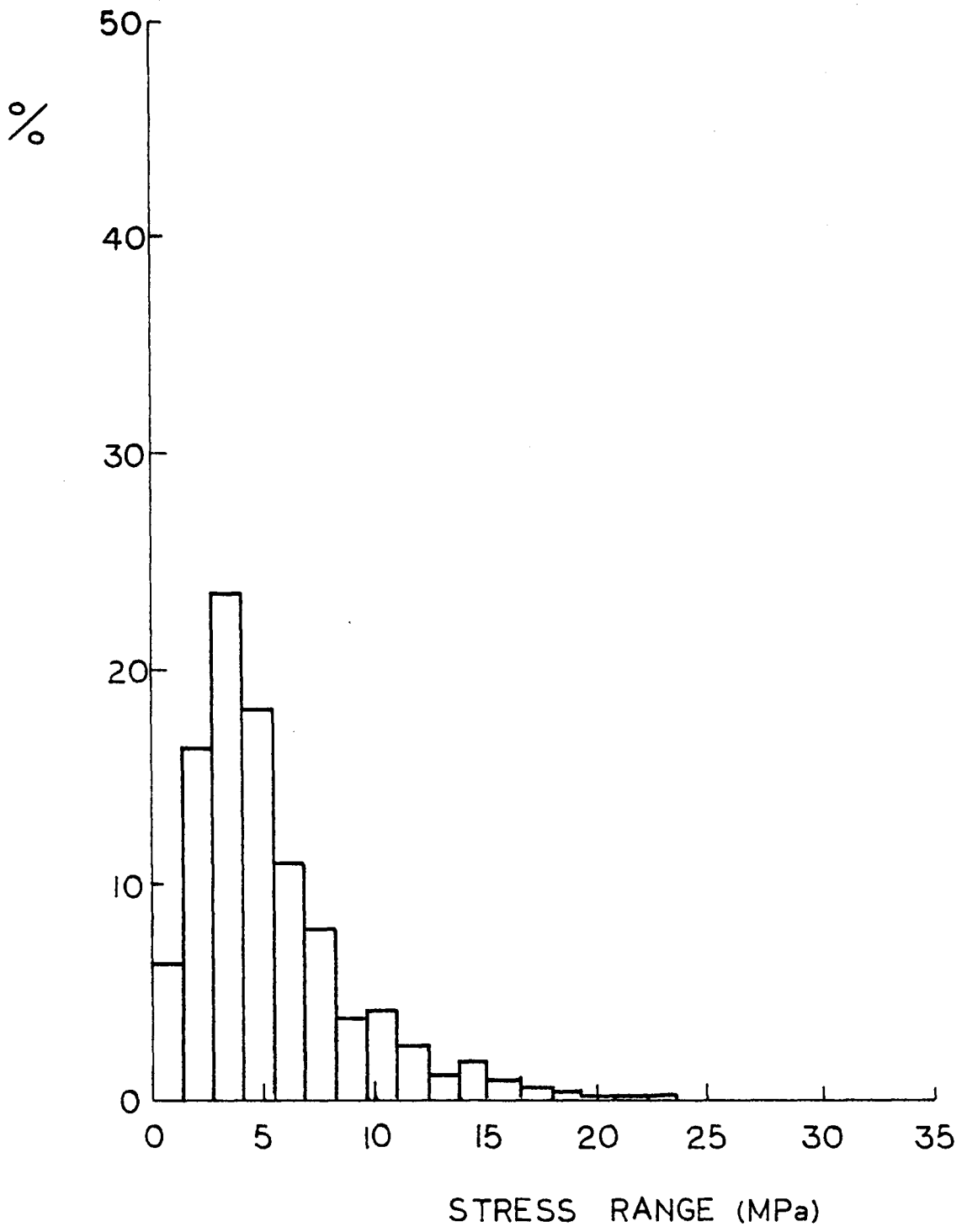

Fig. 12 Histogram for Longitudinal Stiffener Cut-off

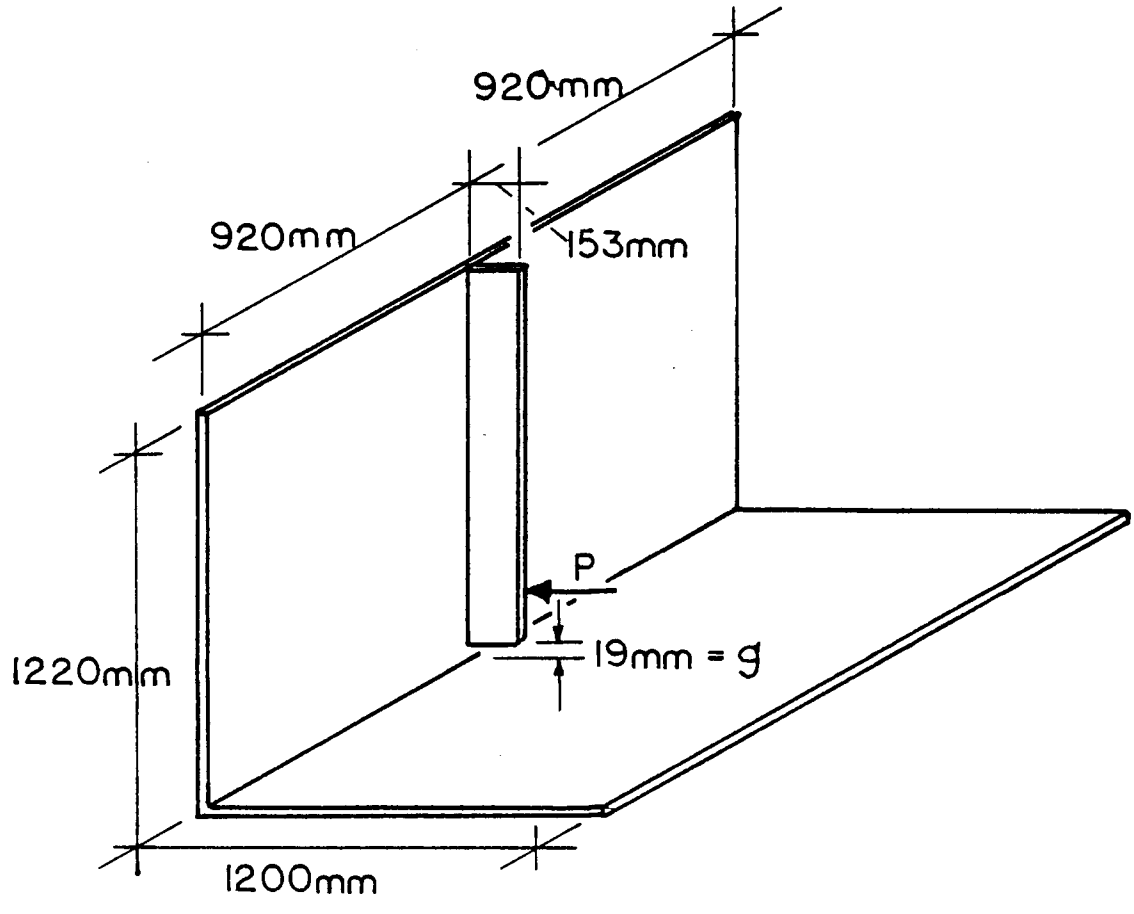

Fig. 13 Transverse Stiffener Detail Substructure

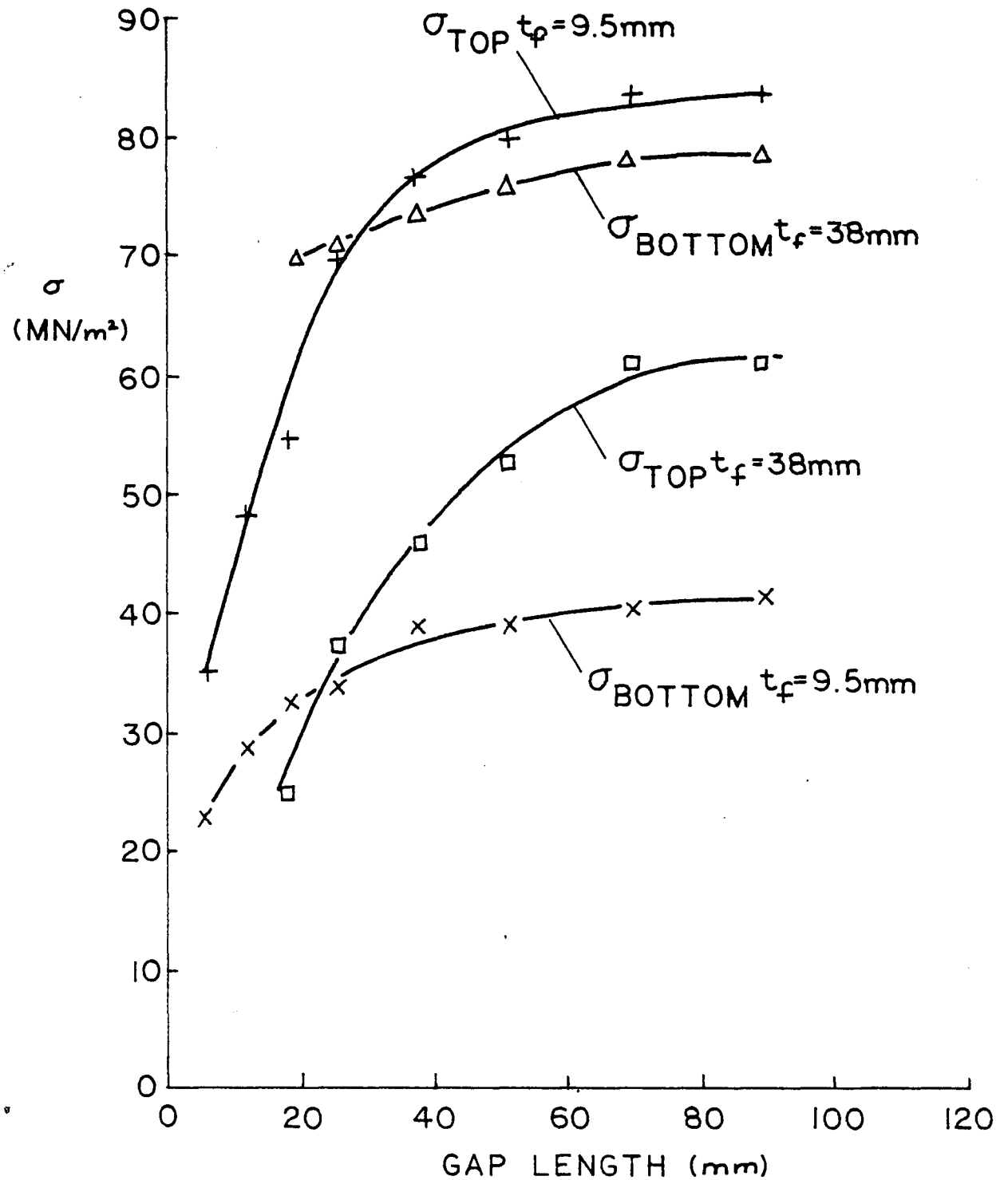

Fig. 14 Results of Parameter Study with Constant Diaphragm Force = 4.4 kN, t_w = 9.5 mm

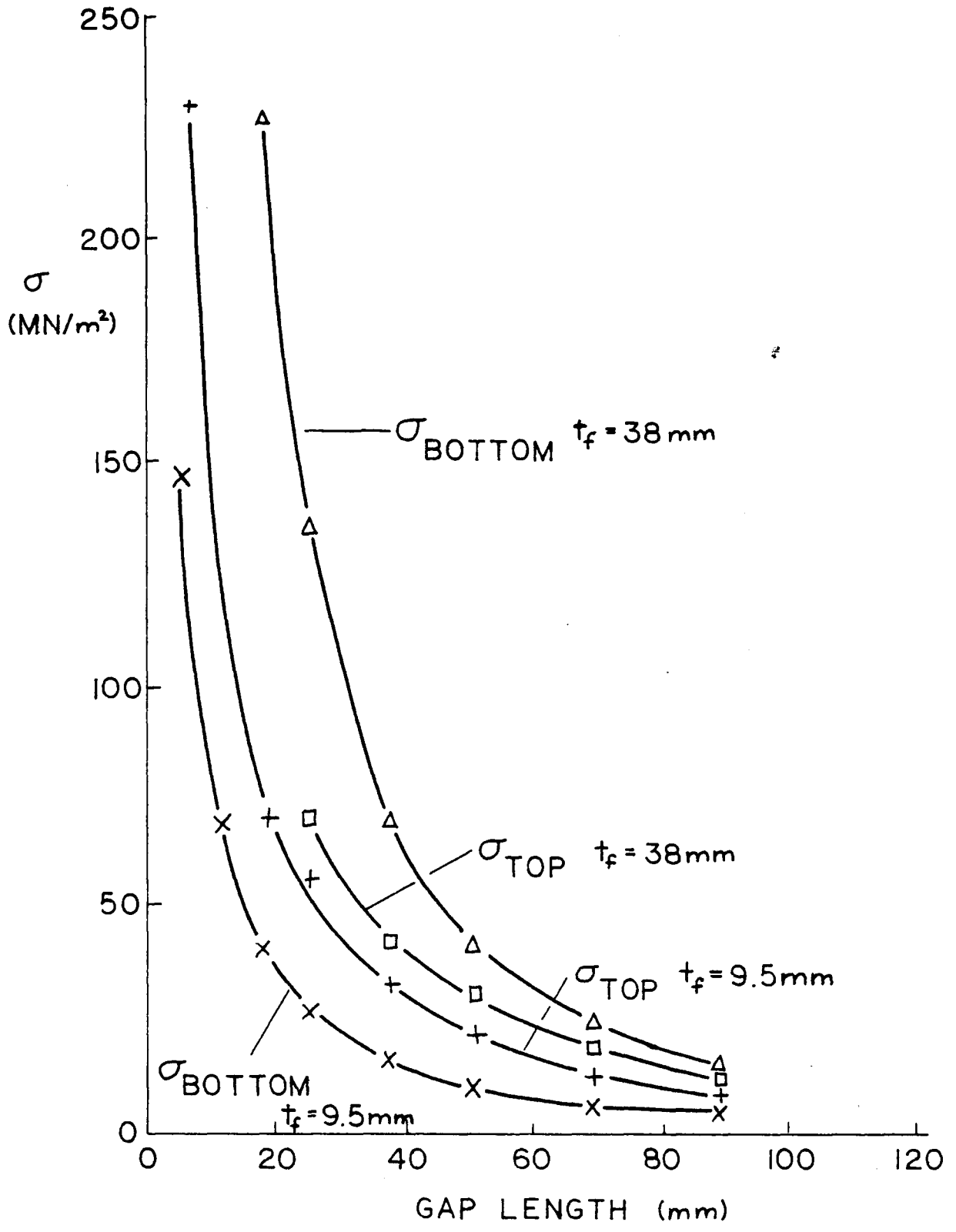

Fig. 15 Results of Parameter Study with Constant Relative Displacement = 2.5×10^{-2} mm, t_w = 9.5 mm

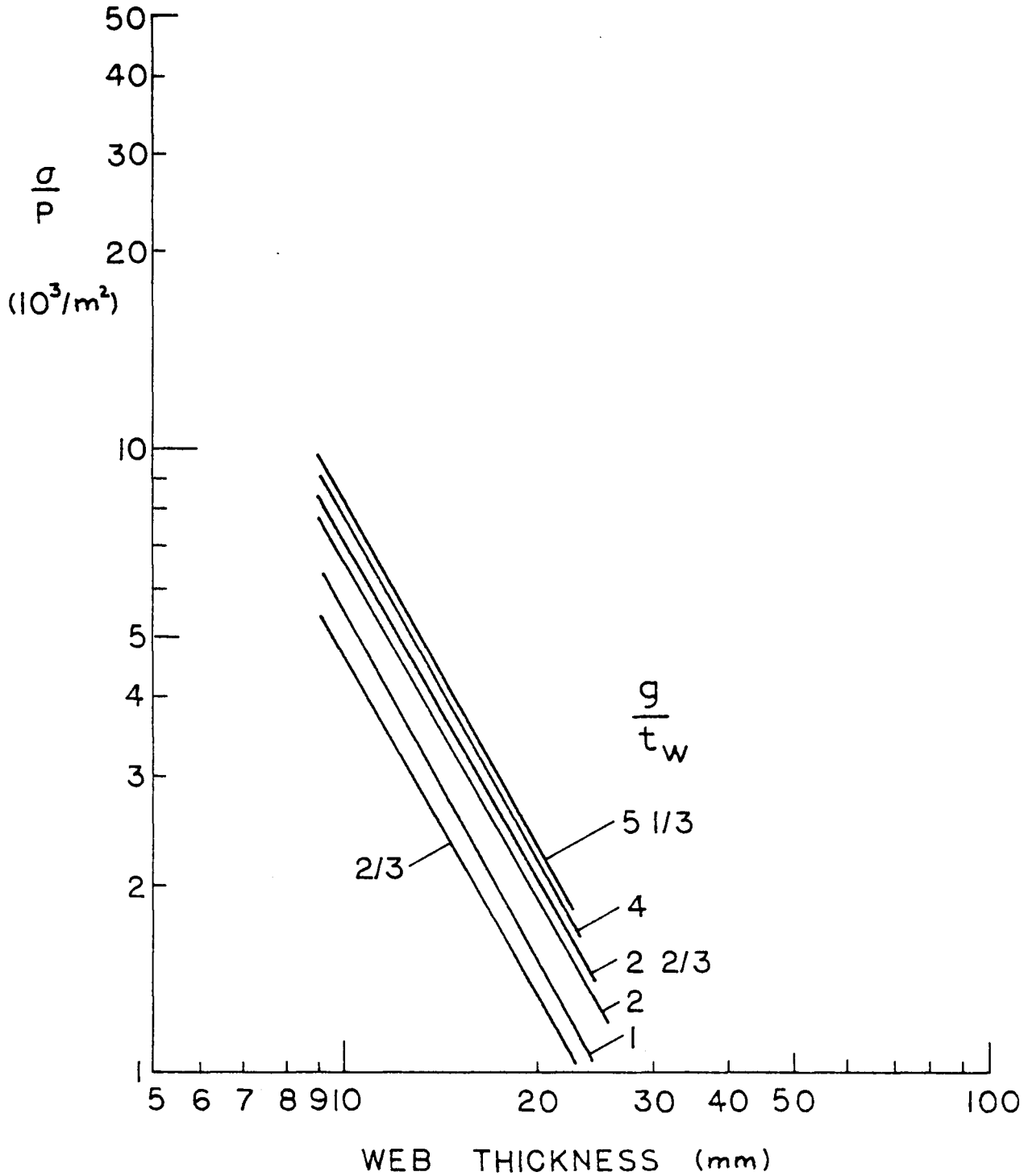

Fig. 16 Maximum Stiffener-Flange Gap Stress, Bottom of Gap, $t_f/t_w = 1.0$

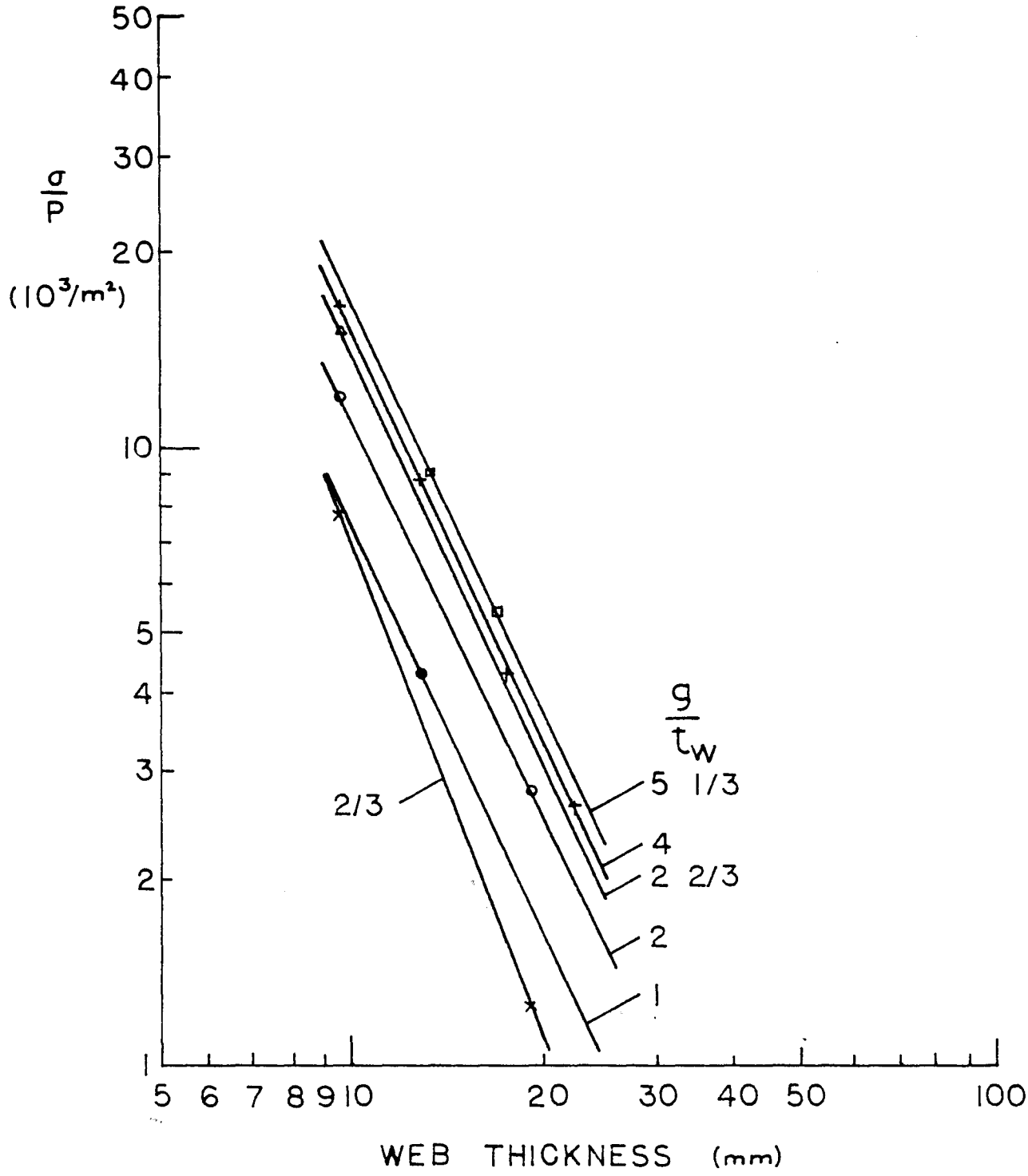

Fig. 17 Maximum Stiffener-Flange Gap Stress, Top of Gap, $t_f/t_w = 1.0$

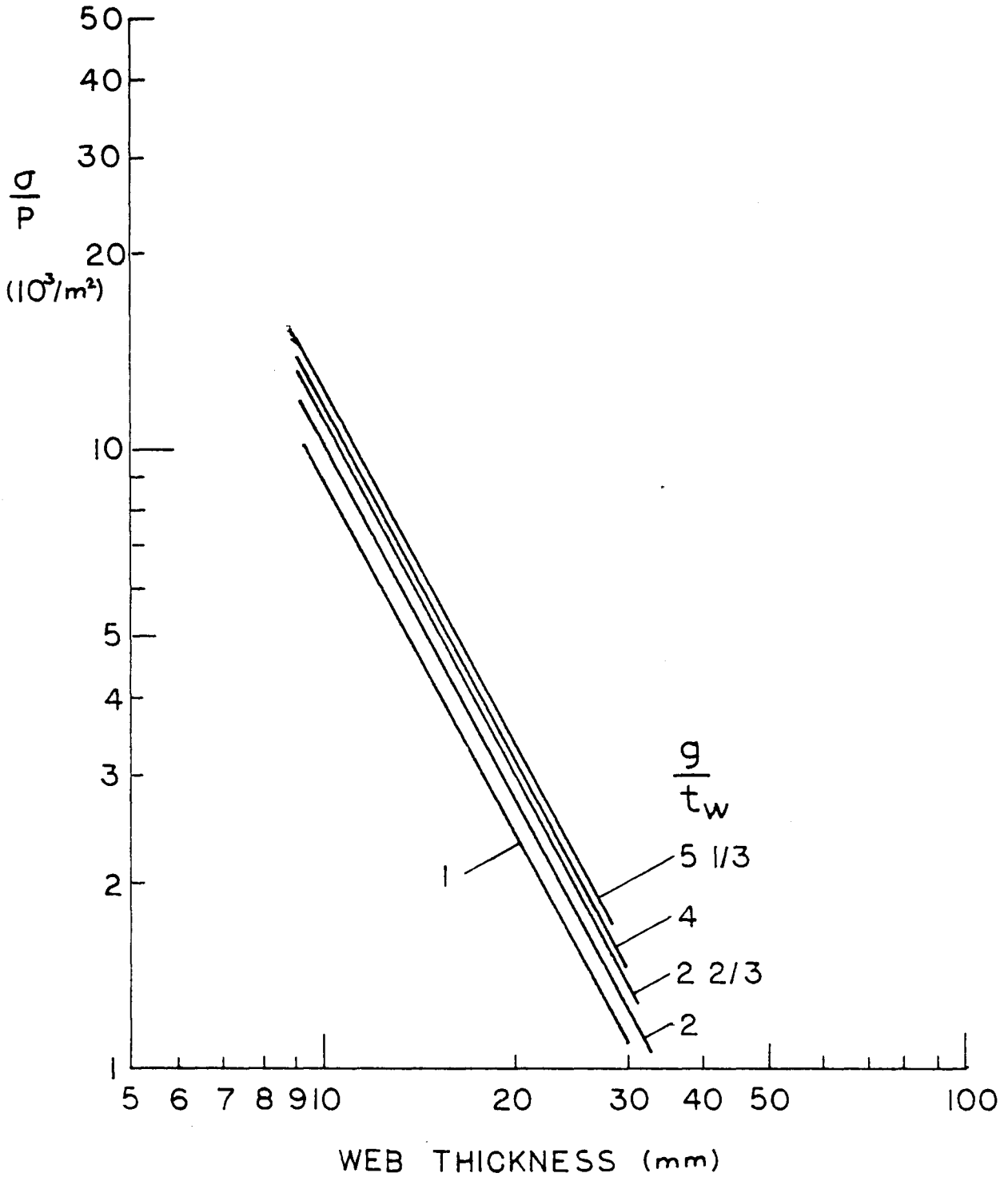

Fig. 18 Maximum Stiffener-Flange Gap Stress, Bottom Gap, $t_f/t_w = 1.5$

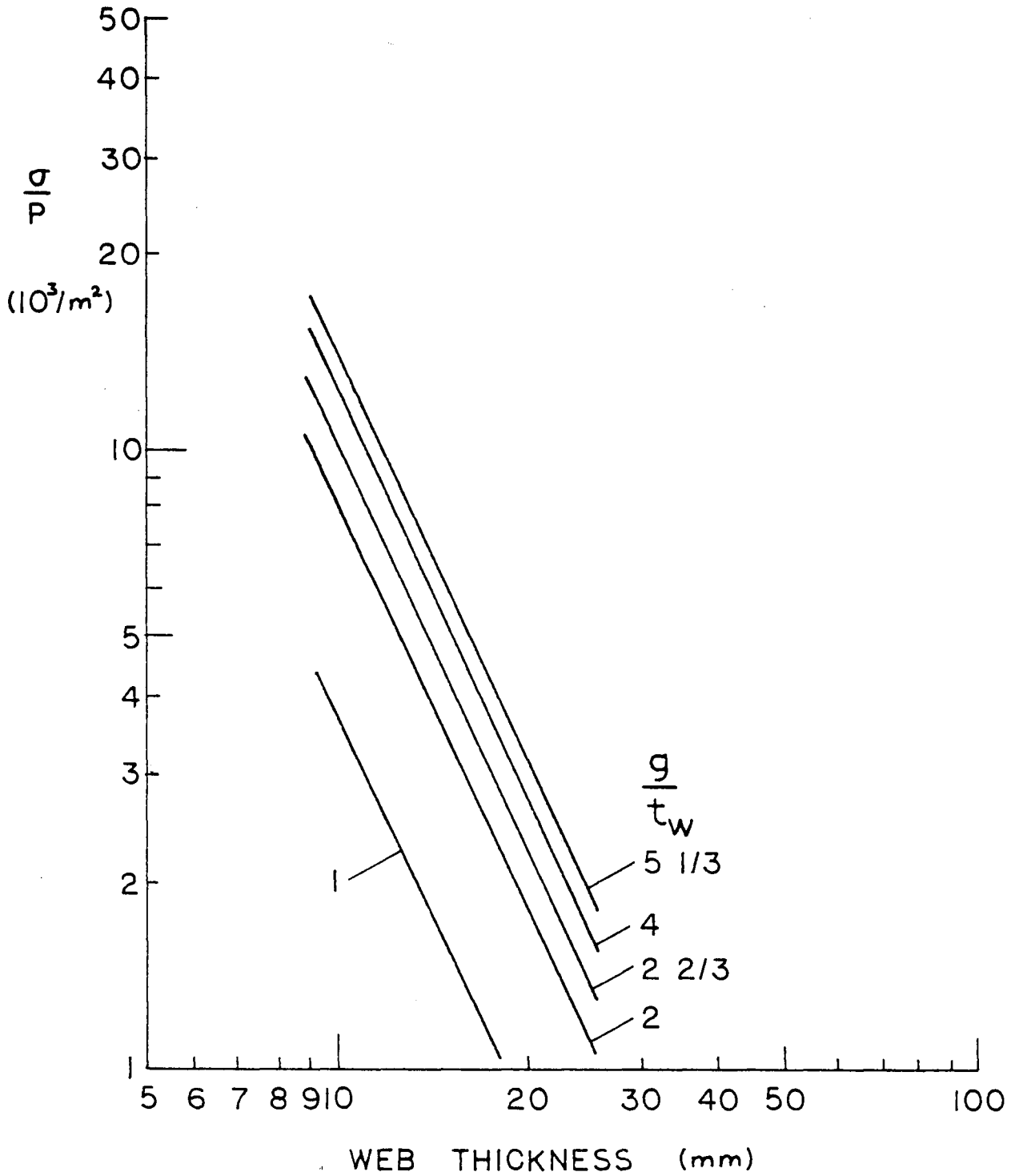

Fig. 19 Maximum Stiffener-Flange Gap Stress, Top of Gap, $t_f/t_w = 1.5$

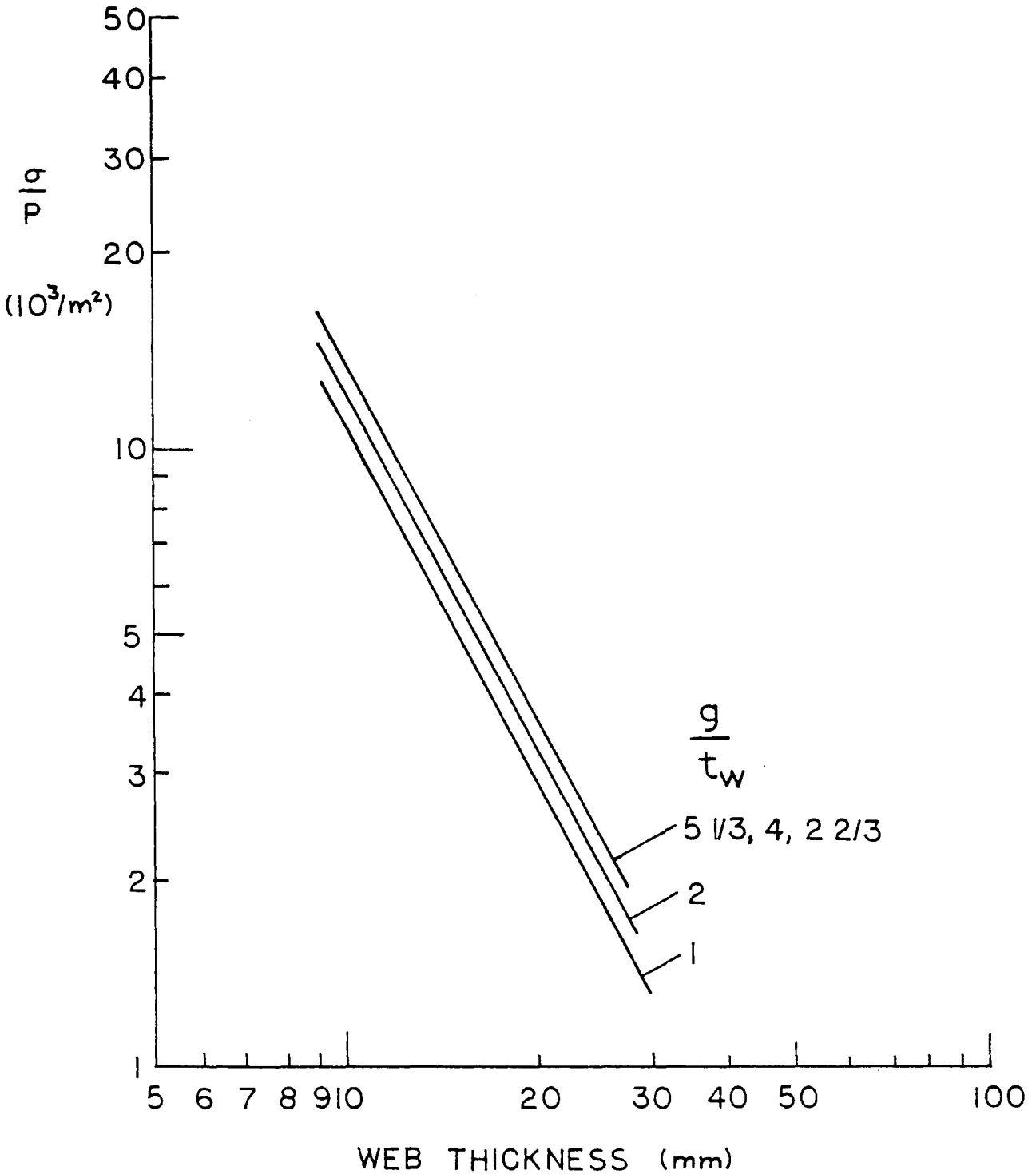

Fig. 20 Maximum Stiffener-Flange Gap Stress, Bottom of Gap, $t_f/t_w = 2.0$

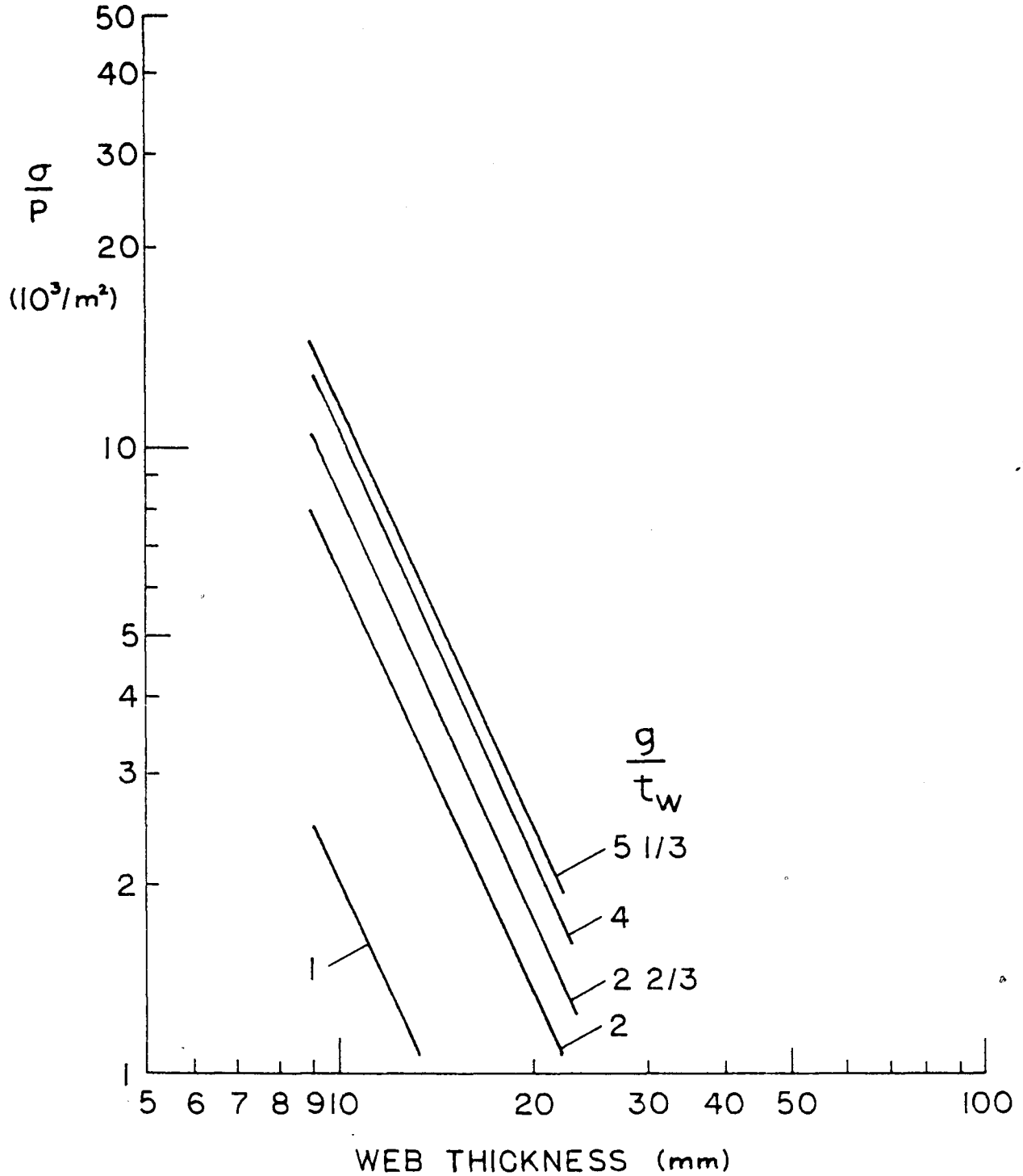

Fig. 21 Maximum Stiffener-Flange Gap Stress, Top of Gap, $t_f/t_w = 2.0$

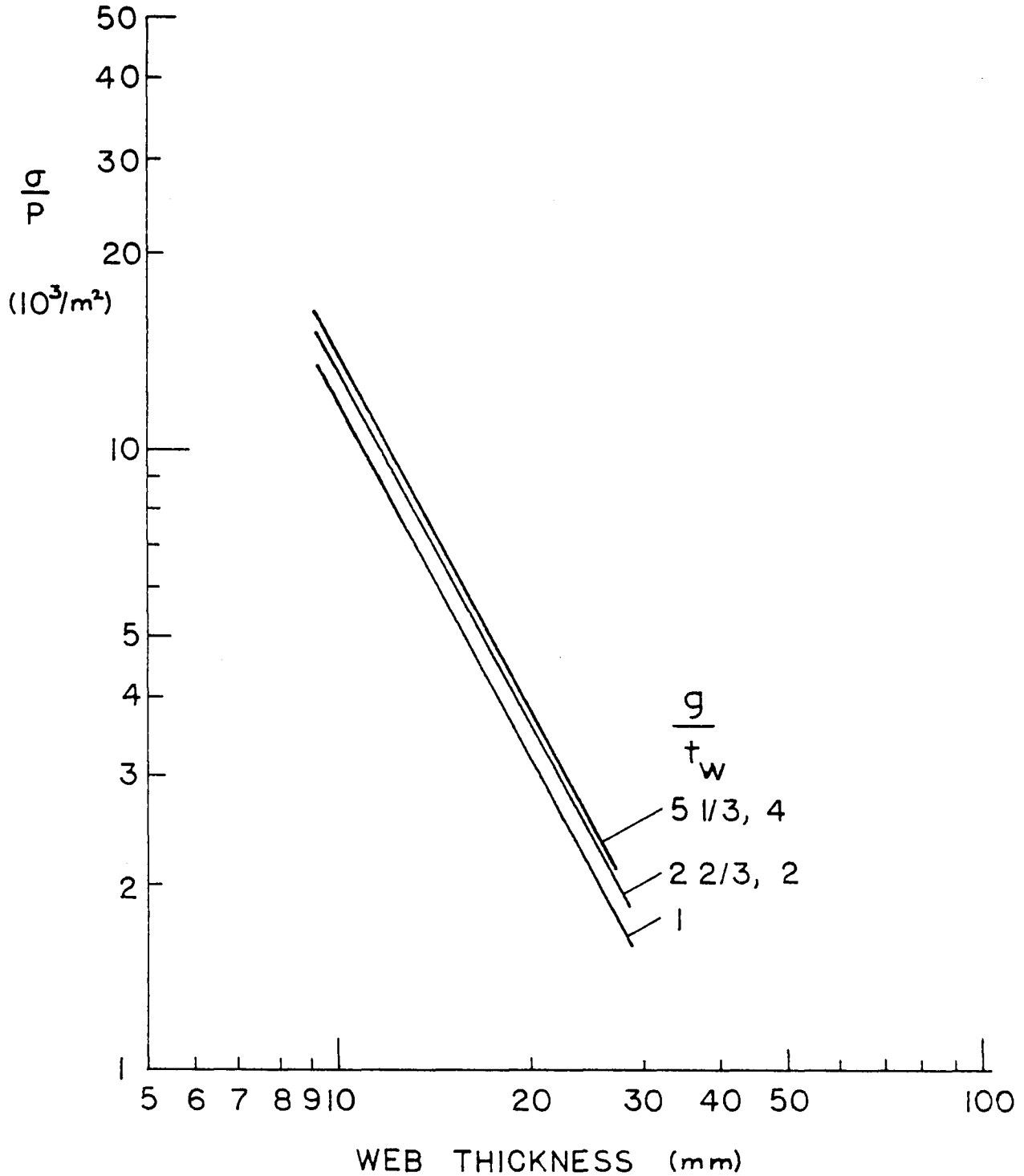

Fig. 22 Maximum Stiffener-Flange Gap Stress, Bottom of Gap, $t_f/t_w = 2.5$

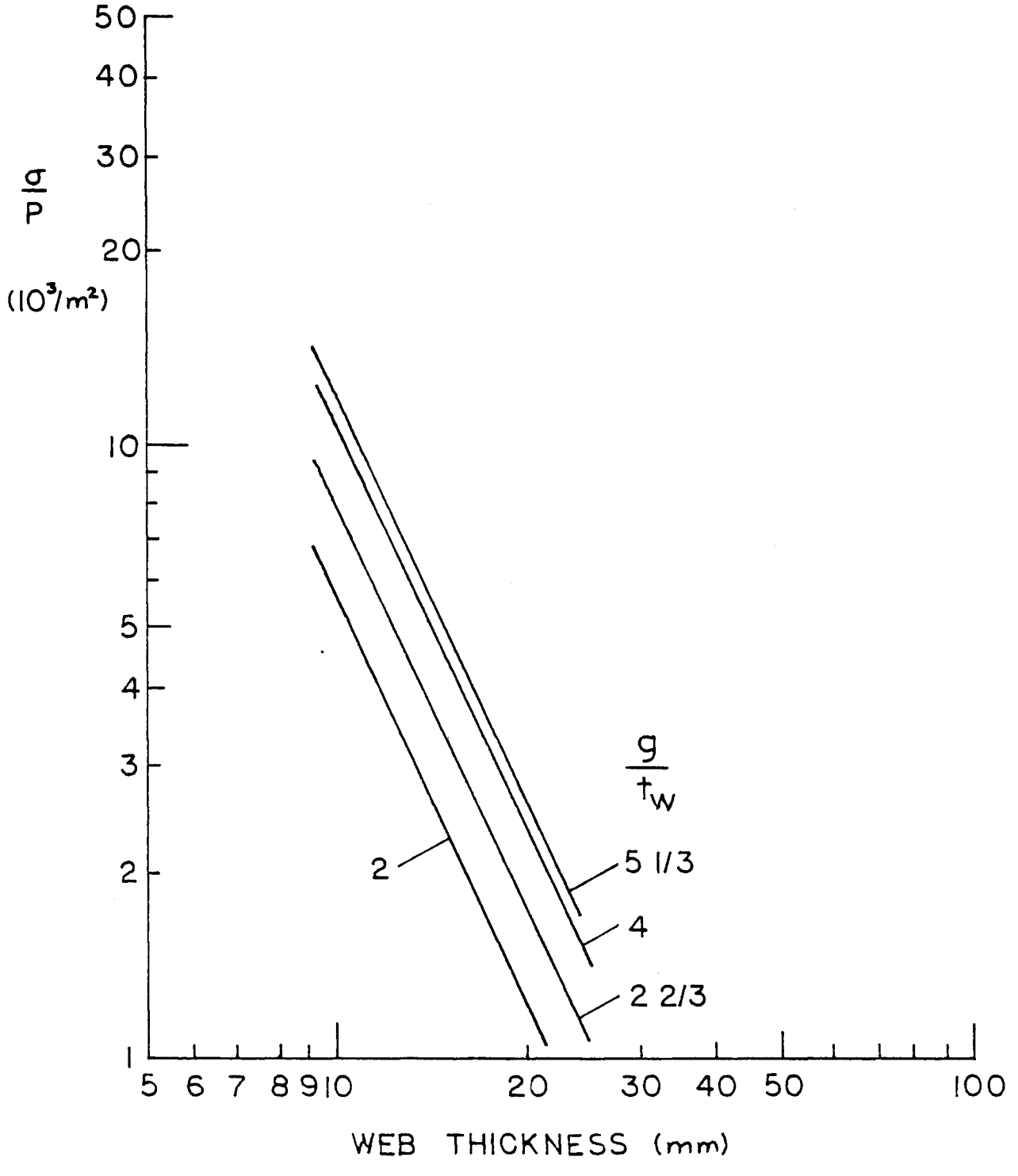

Fig. 23 Maximum Stiffener-Flange Gap Stress, Top of Gap, $t_f/t_w = 2.5$

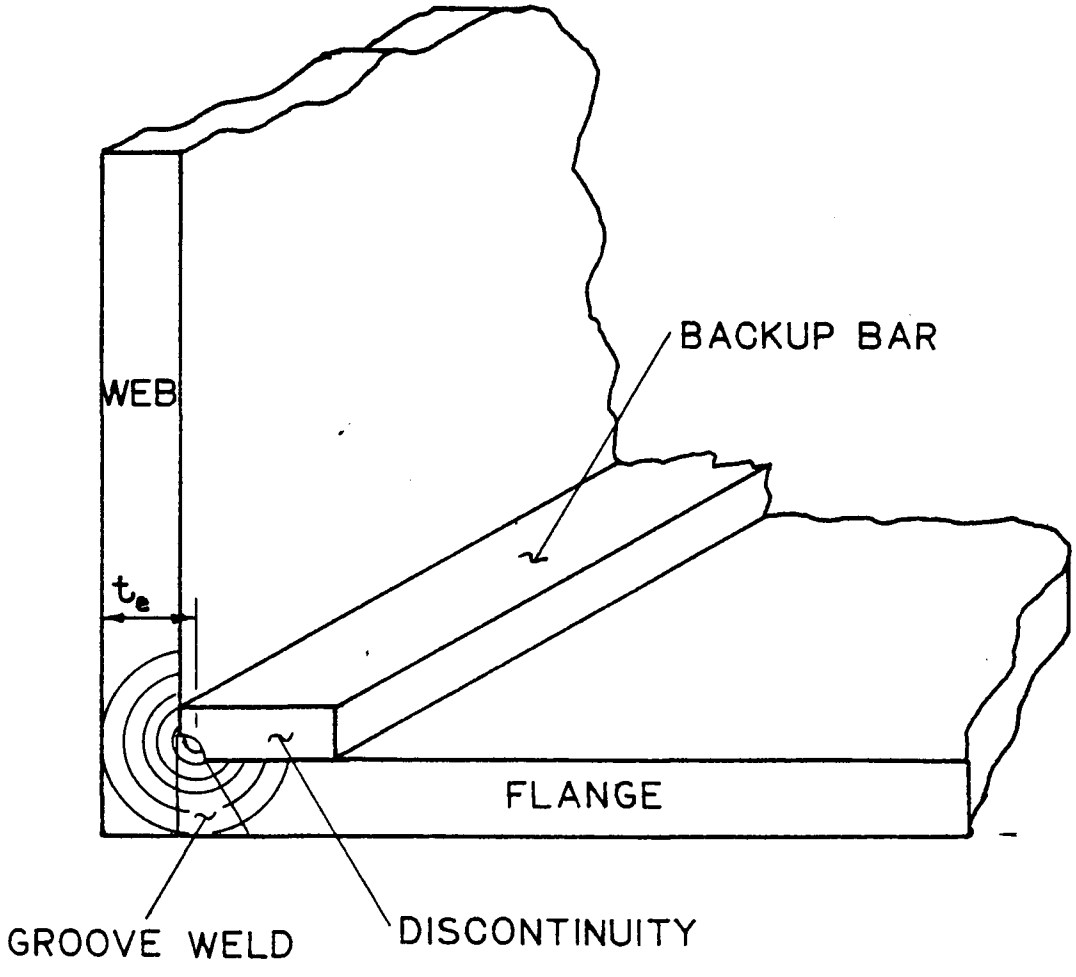

Fig. 24 Discontinuous Backup Bar Detail

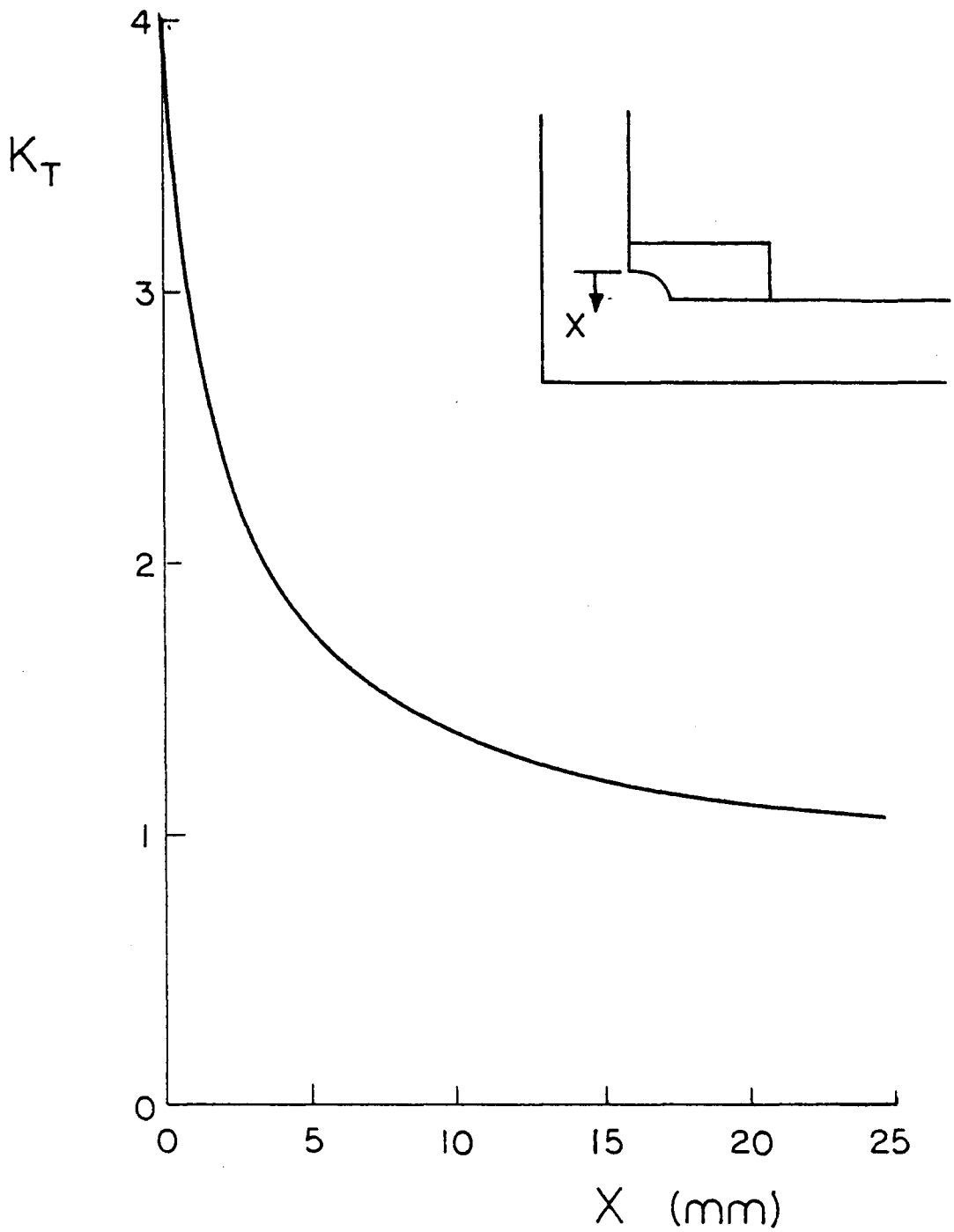

Fig. 25 Stress Concentration Decay Curve

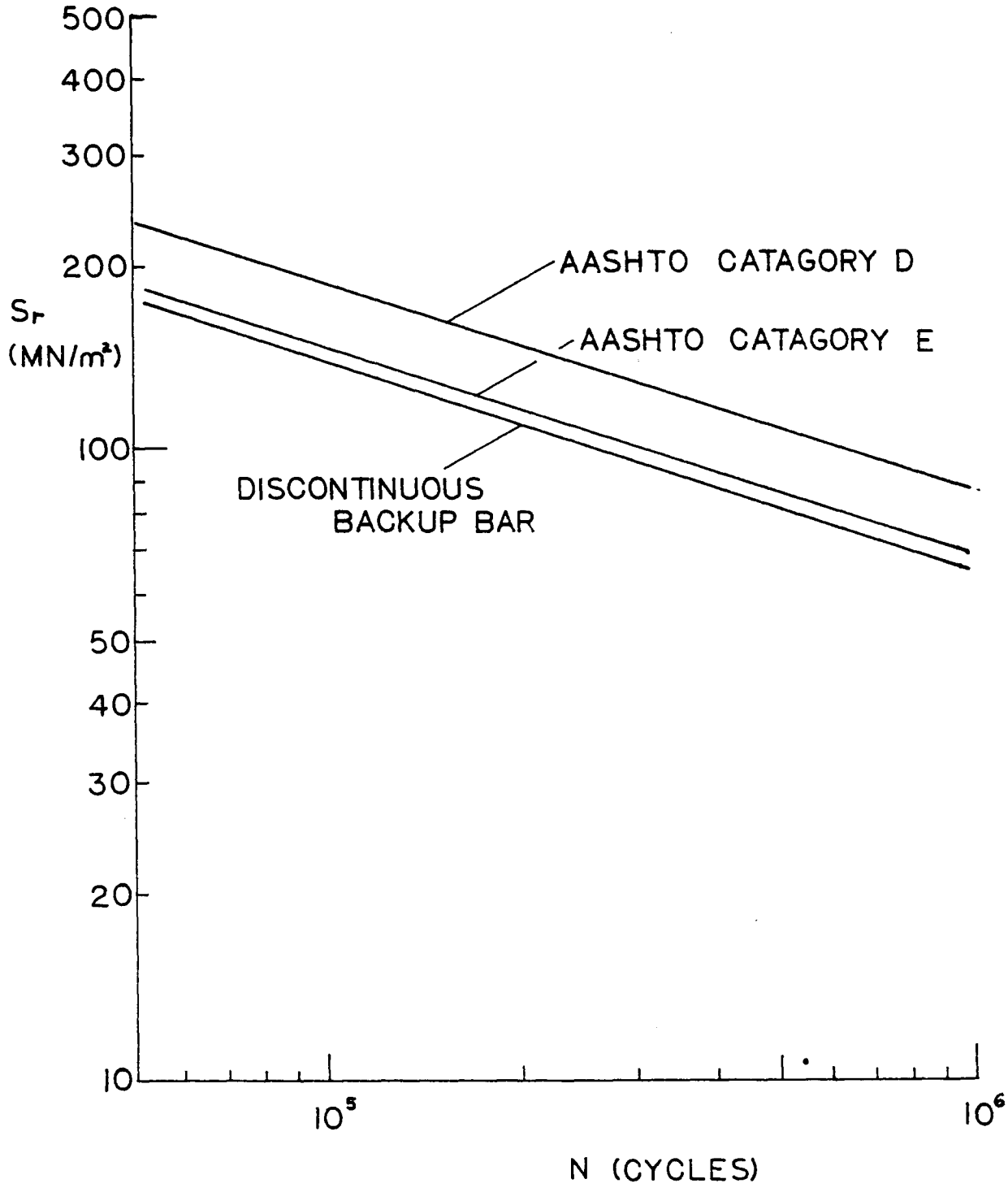

Fig. 26 Estimate of Fatigue Life of Discontinuous Backup Bar Detail

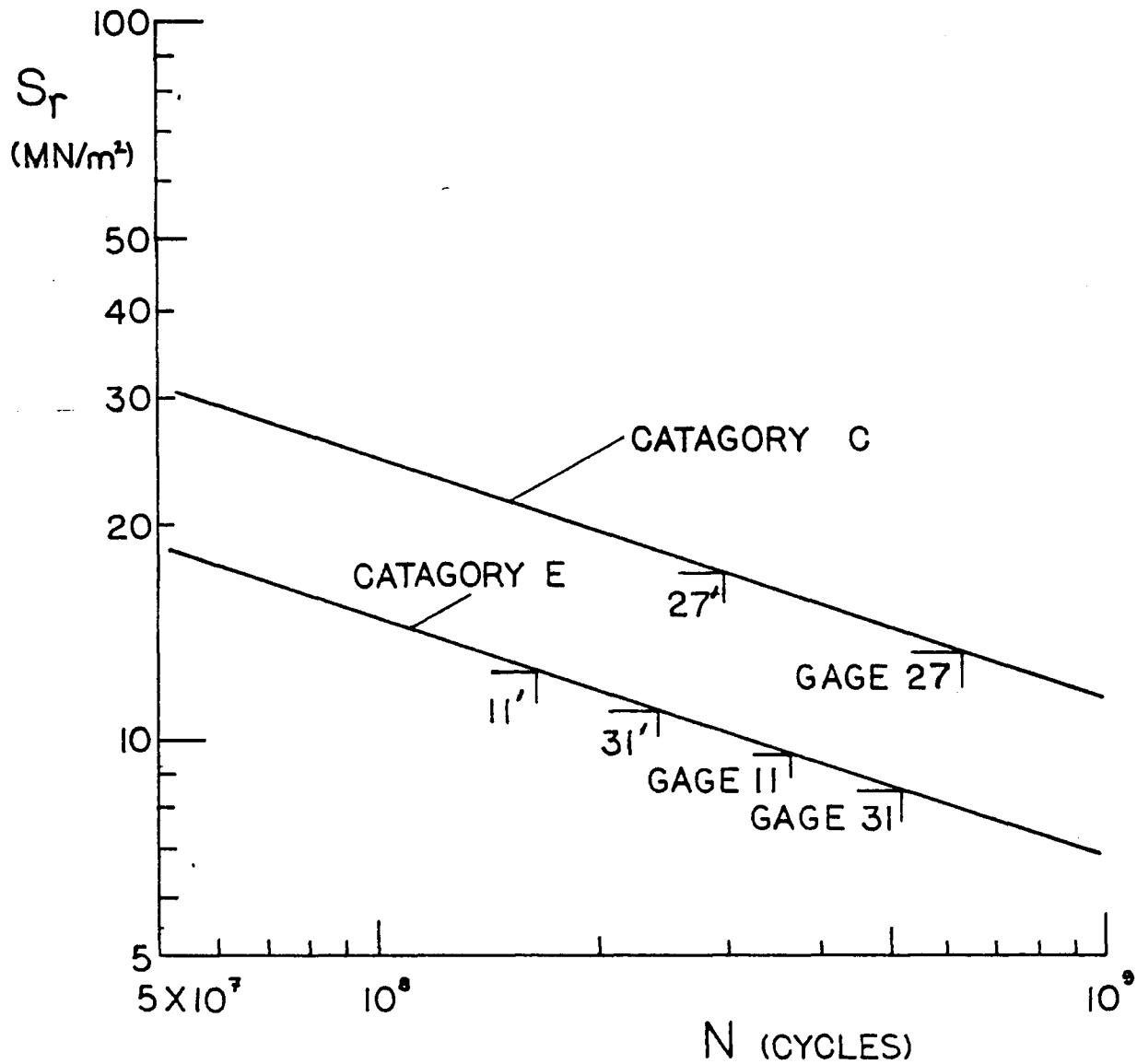

Fig. 27 S-N Curve Showing Estimated Fatigue Life of Details

Primed Gage Numbers Account for Future Load Increase of 30%

REFERENCES

1. Bowers, D. G.
   LOADING HISTORY SPAN NO. 10, YELLOW MILL POND BRIDGE I-95, BRIDGEPORT, CONNECTICUT,
   Highway Research Record No. 428, Transportation Research Board, 1973.

2. Fisher, J. W., Yen, B. T., Marchica, N. V.
   FATIGUE DAMAGE IN THE LEHIGH CANAL BRIDGE,
   Fritz Engineering Laboratory Report No. 386.1, Lehigh University, November 1974.

3. Marchica, N. V., Yen, B. T., Fisher, J. W.
   STRESS HISTORY STUDY OF THE ALLEGHENY RIVER BRIDGE (PENNSYLVANIA TURNPIKE),
   Fritz Engineering Laboratory Report No. 386.3, Lehigh University, May 1974.

4. Ostapenko, A. et al
   A STUDY OF THE PRESIDENT COSTA E SILVA BRIDGE DURING CONSTRUCTION AND SERVICE (STEEL STRUCTURE),
   Fritz Engineering Laboratory Report No. 397.6, Lehigh University, March 1976.

5. Swanson, S. R.
   RANDOM LOAD FATIGUE TESTING: A STATE OF THE ART SURVEY,
   ASTM, Materials Research and Standards, Vol. 8, No. 4, April 1968.

6. Miner, M. A.
   CUMULATIVE DAMAGE IN FATIGUE,
   Journal of the Applied Mechanics, Vol. 12, No. 1, September 1945.

7. Bathe, K., Wilson, E. L., Peterson, F. E.
   SAP IV, A STRUCTURAL ANALYSIS PROGRAM FOR STATIC AND DYNAMIC RESPONSE OF LINEAR SYSTEMS,
   Earthquake Engineering Research Center Report No. EERC 73-11, University of California, Berkeley, June 1973.

REFERENCES (continued)

8. American Institute of Steel Construction
   MANUAL OF STEEL CONSTRUCTION,
   AISC, New York, N. Y., 1973.

9. American Association of State Highway Officials
   STANDARD SPECIFICATIONS FOR HIGHWAY BRIDGES,
   AASHO, Washington, D. C., 1973.

10. American Welding Society
    STRUCTURAL WELDING CODE,
    AWS, Miami, Florida, 1975.

11. Paris, P. C.
    FATIGUE - AN INTERDISCIPLINARY APPROACH,
    Proceedings 10th Sagamore Conference, page 107,
    Syracuse University Press, Syracuse, New York, 1964.

12. Zettlemoyer, N.
    STRESS CONCENTRATION AND FATIGUE OF WELDED DETAILS,
    Unpublished Ph.D. Dissertation, Lehigh University, 1976.

13. Hertzberg, R. W.
    DEFORMATION AND FRACTURE MECHANICS OF ENGINEERING MATERIALS,
    John Wiley & Sons, Inc., New York, N. Y., 1976.

14. Batcheler, R. P.
    STRESS CONCENTRATION AT BACKUP BAR DISCONTINUITIES,
    Unpublished Special Report, Lehigh University, 1976.

15. Fisher, J. W.
    GUIDE TO 1974 AASHTO FATIGUE SPECIFICATIONS,
    American Institute of Steel Construction,
    New York, N. Y., 1974.

APPENDIX A

STRESS RANGE HISTOGRAMS AT VARIOUS GAGE LOCATIONS

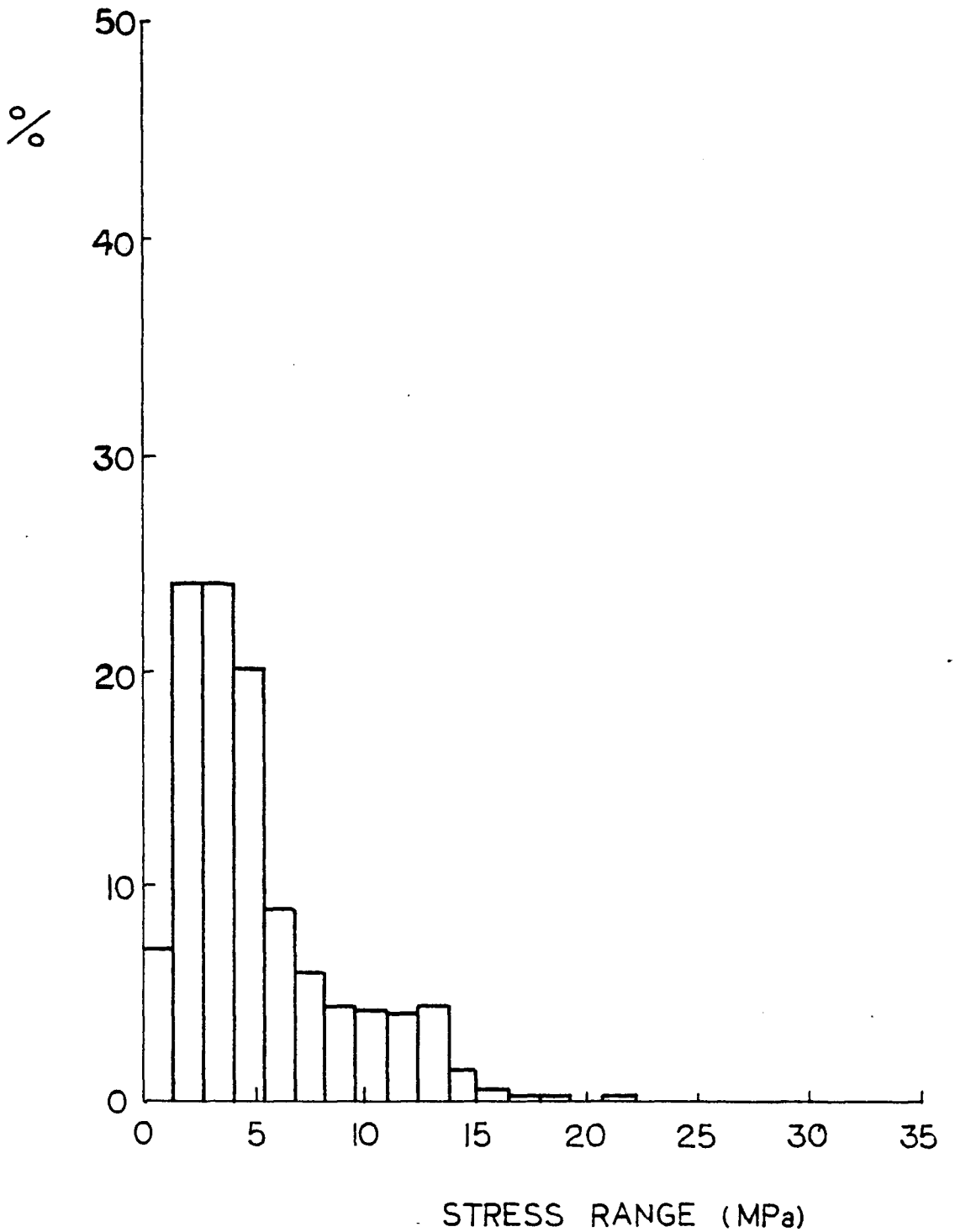

Fig. A.1 Histogram for Gage 5

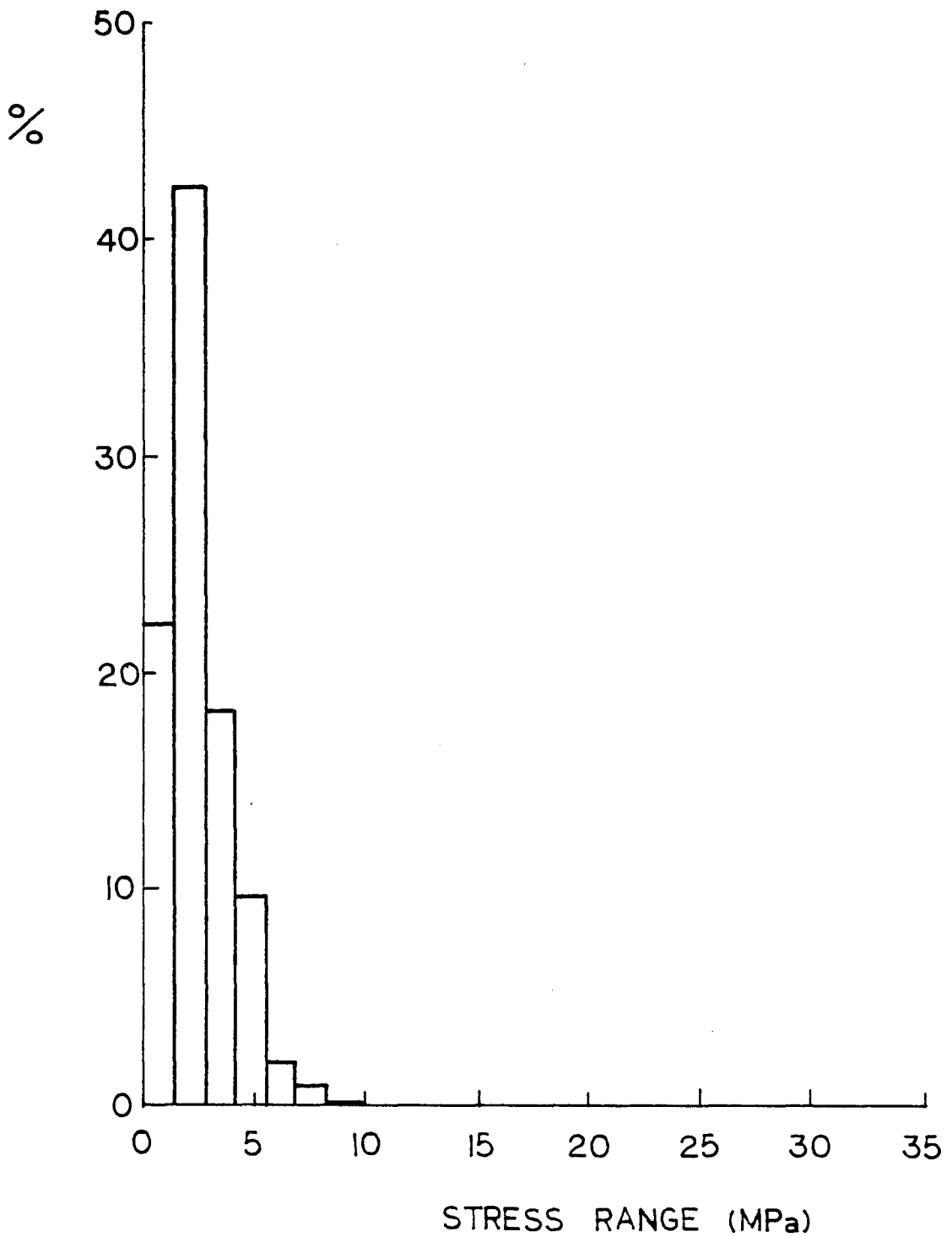

Fig. A.2 Histogram for Gage 8

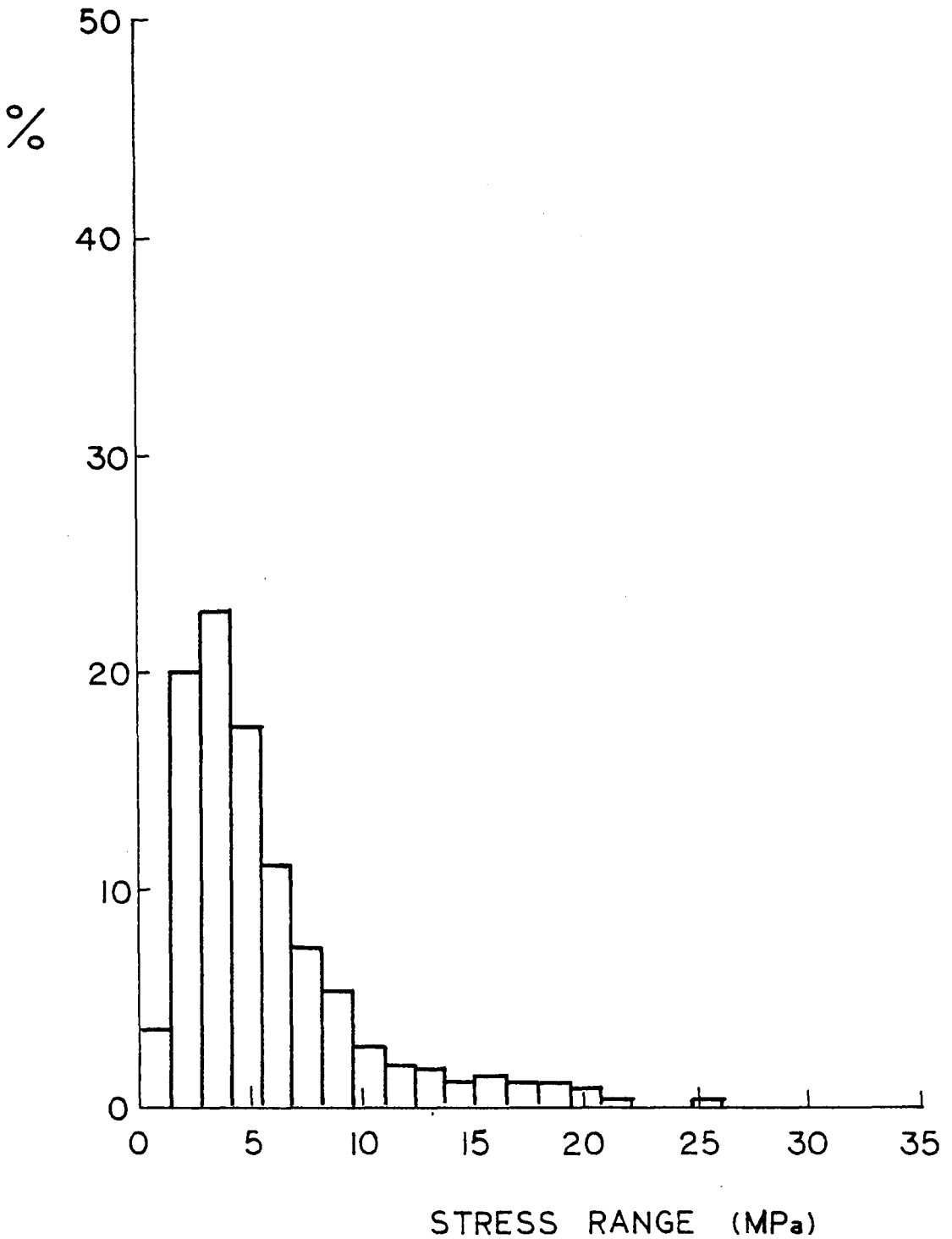

Fig. A.3 Histogram for Gage 12

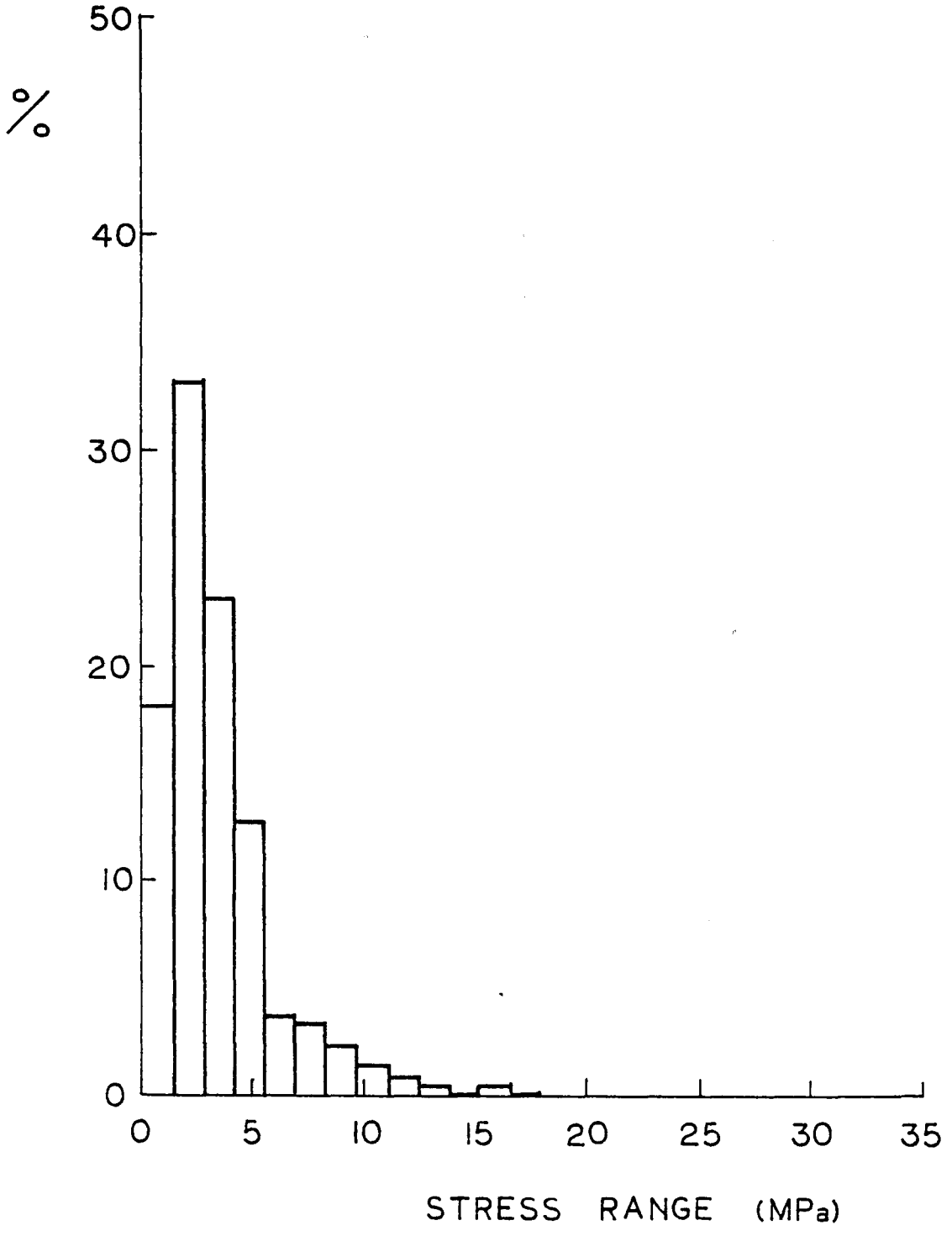

Fig. A.4 Histogram for Gage 13

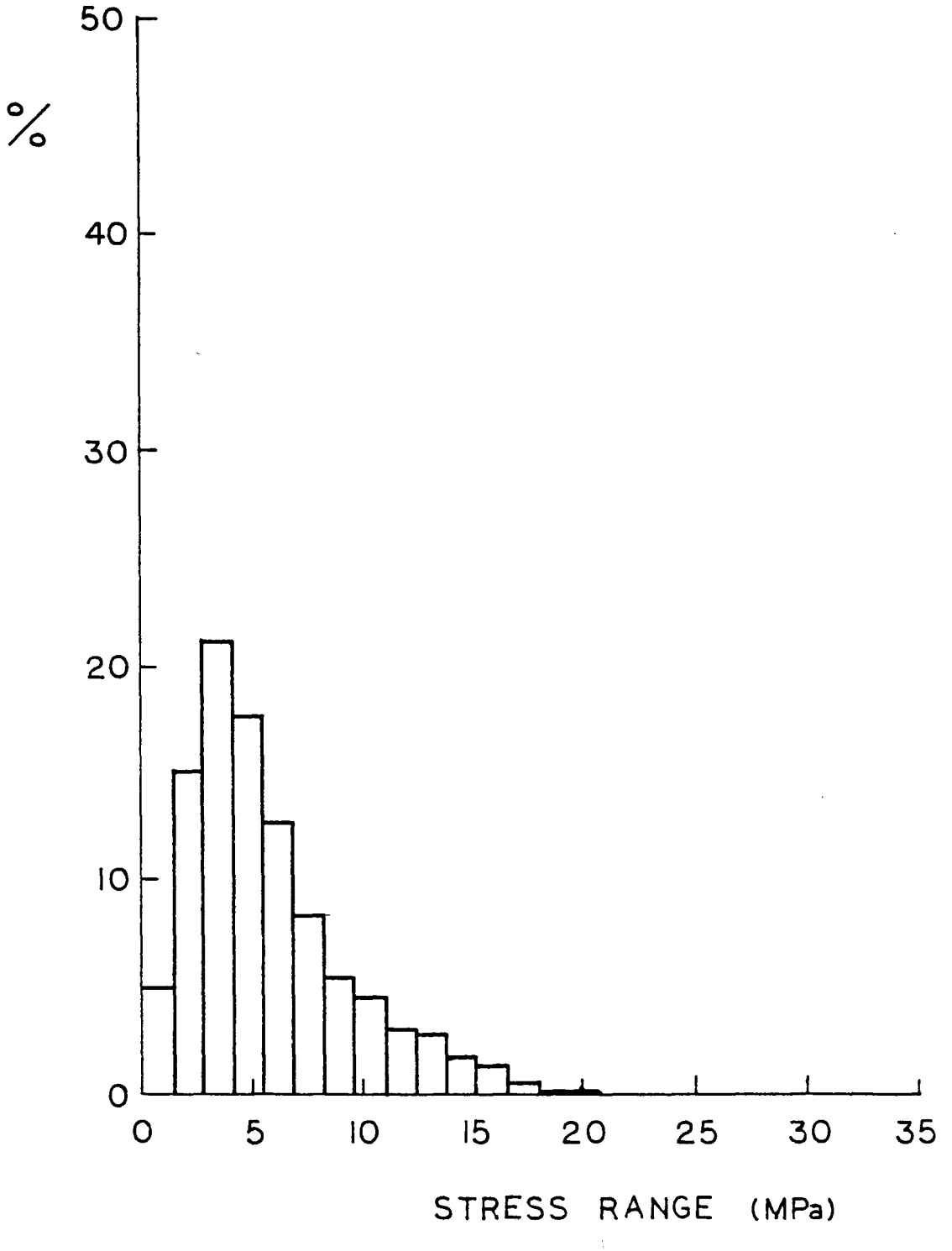

Fig. A.5 Histogram for Gage 19

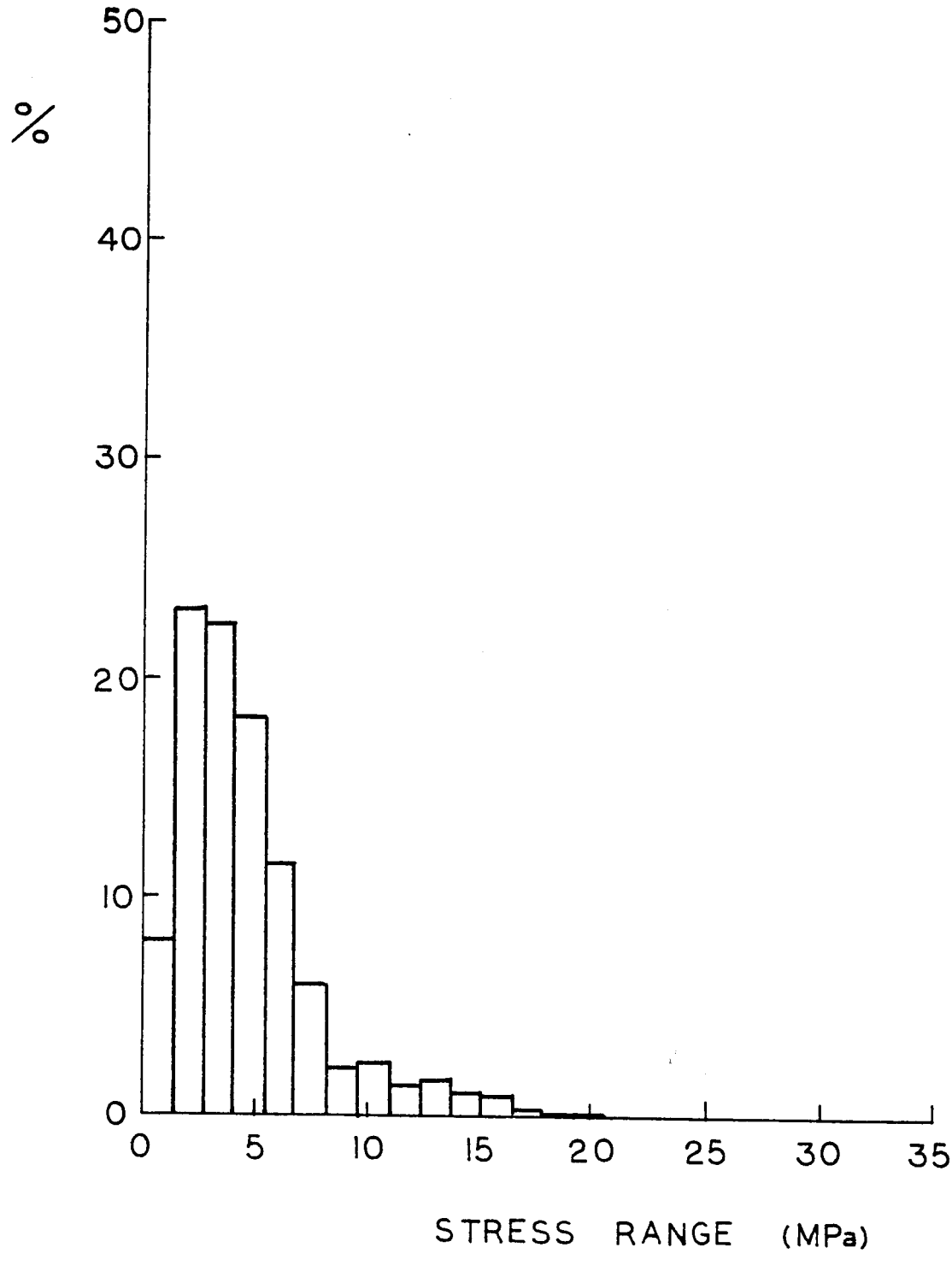

Fig. A.6 Histogram for Gage 21

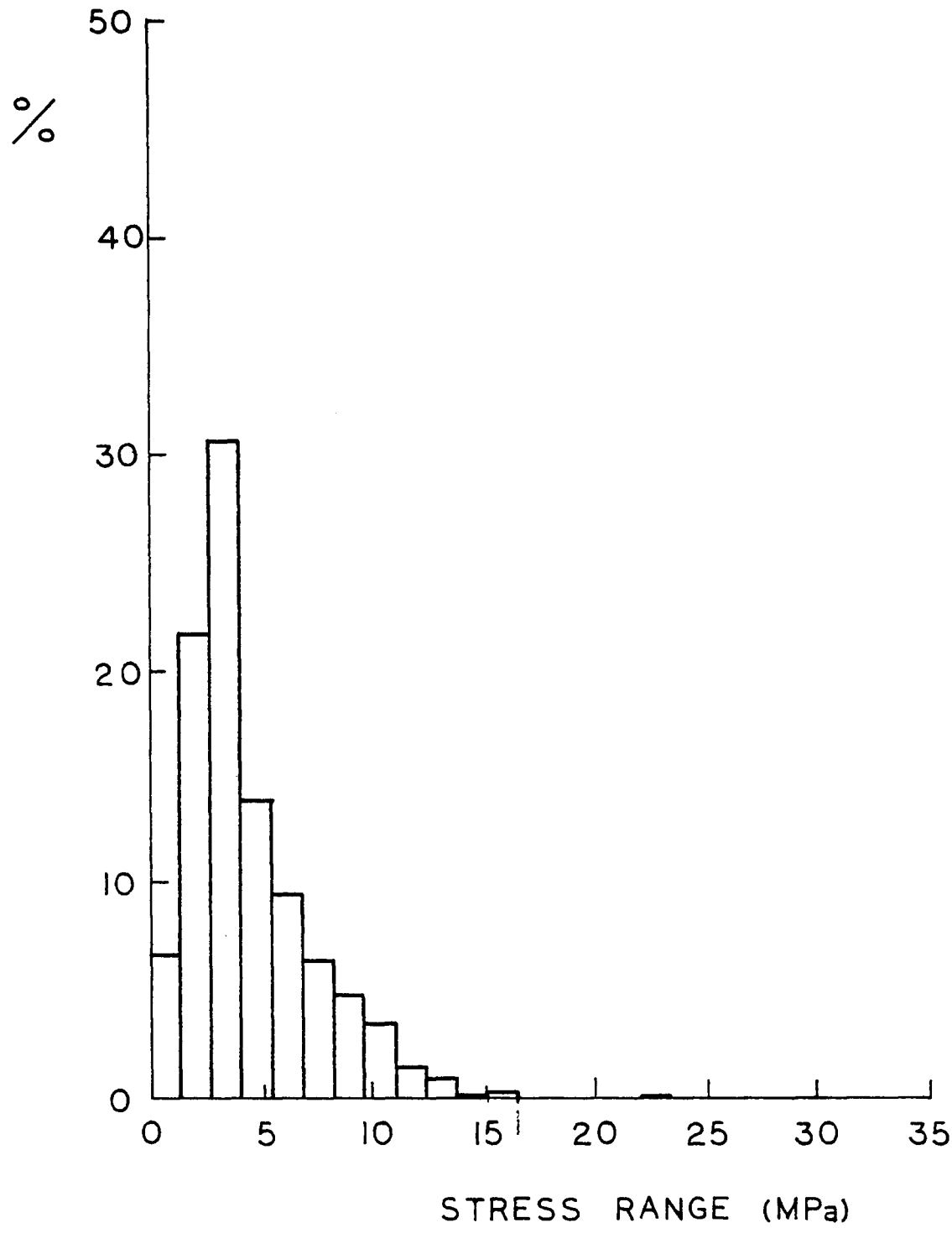

Fig. A.7 Histogram for Gage 26

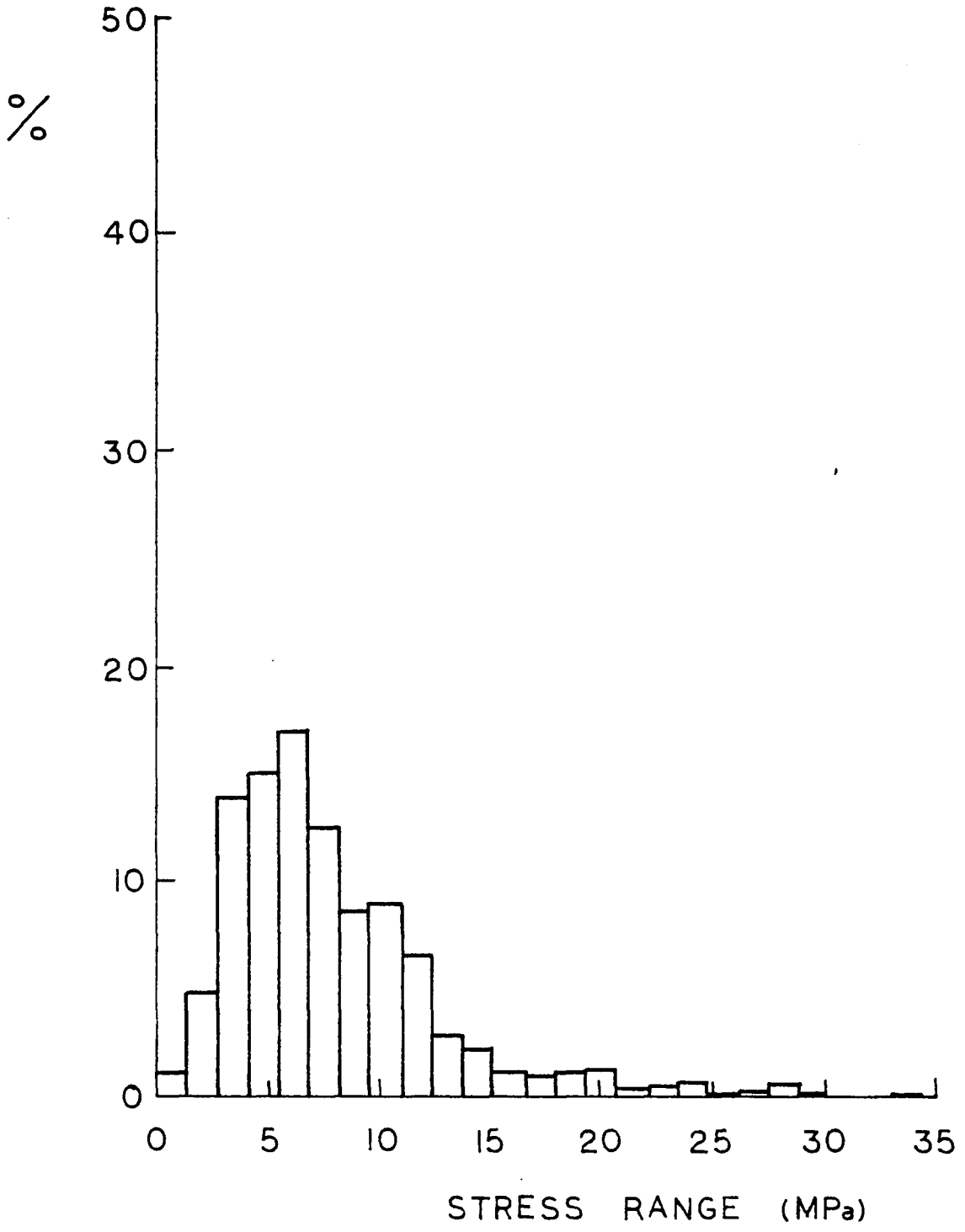

Fig. A.8 Histogram for Gage 27

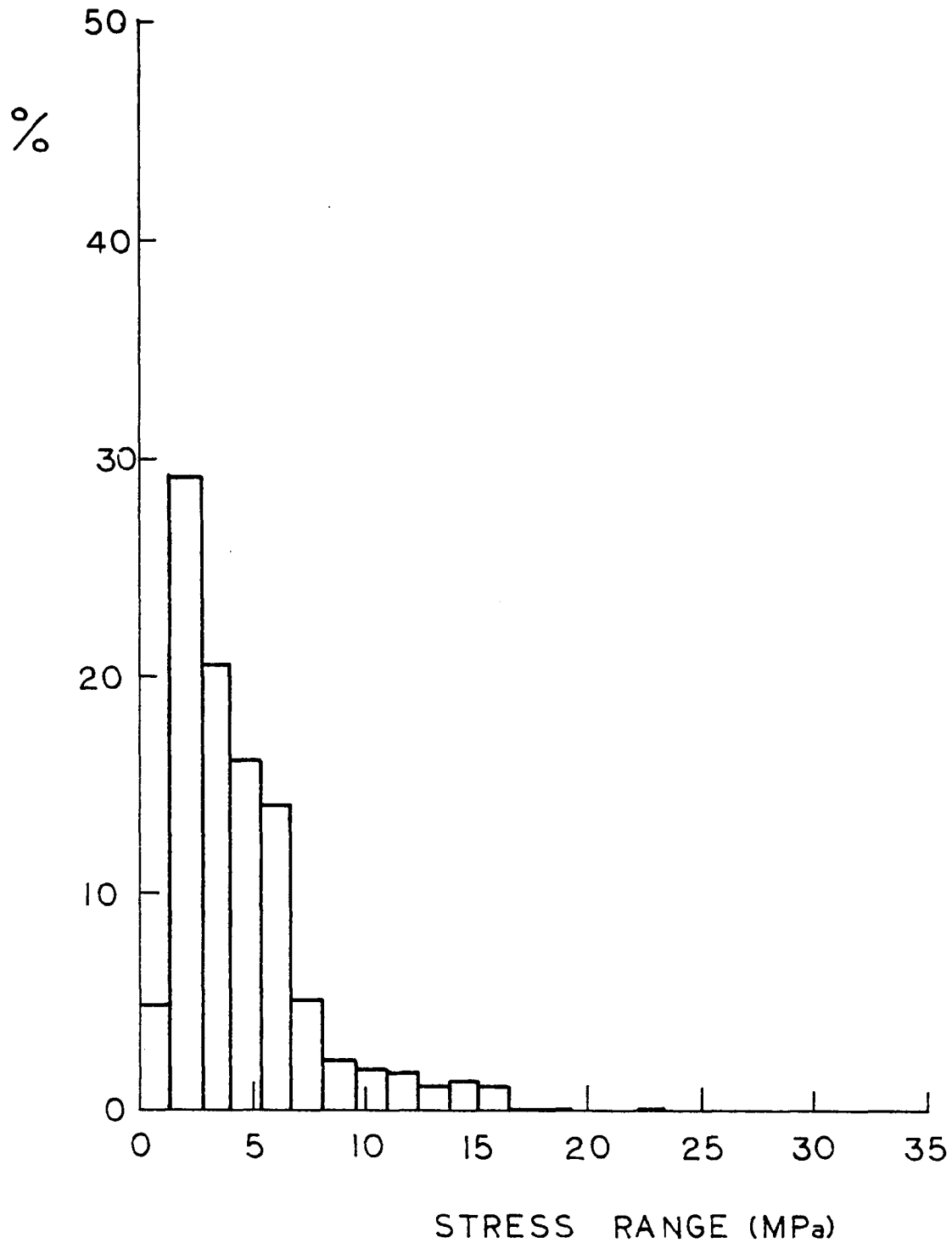

Fig. A.9 Histogram for Gage 31

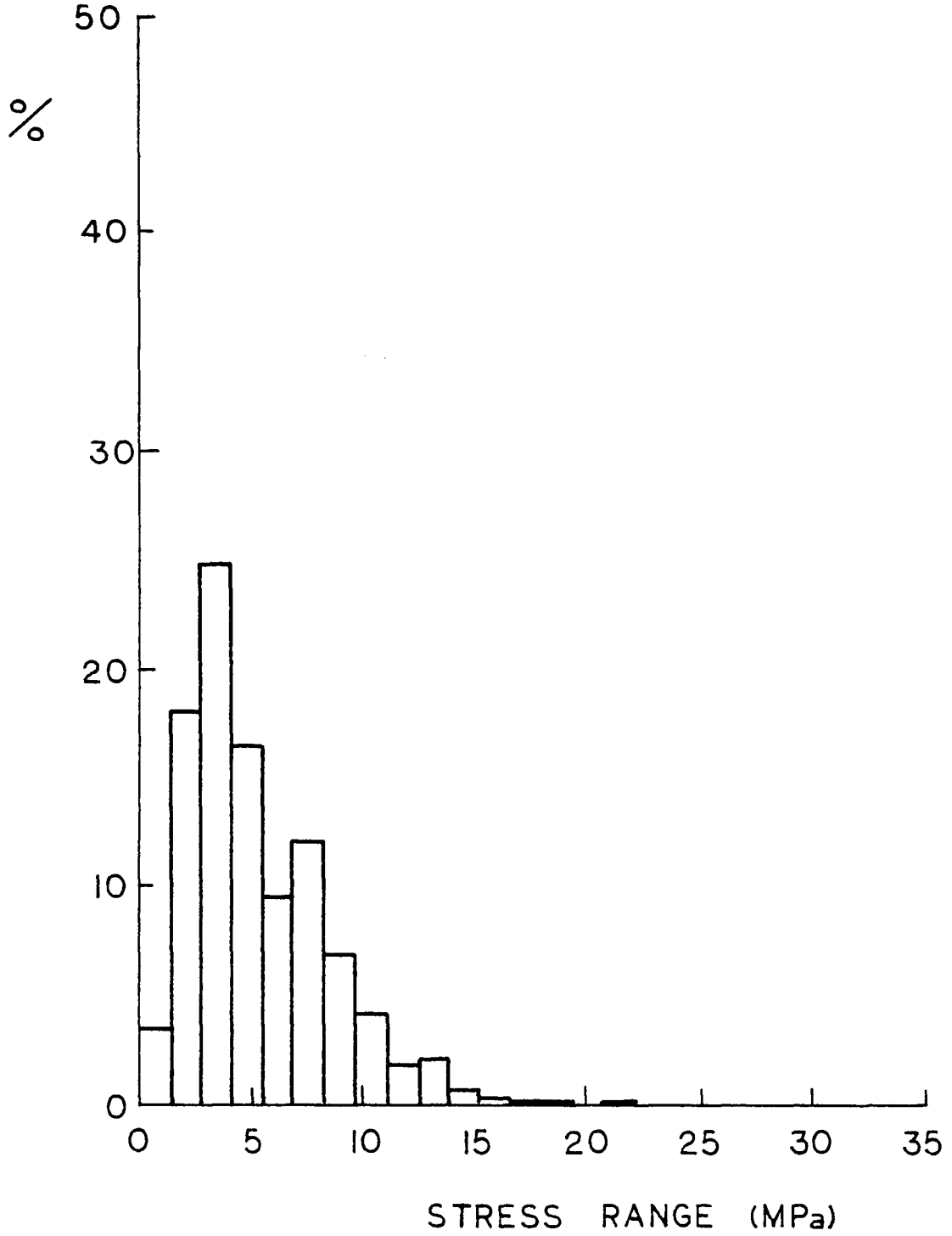

Fig. A.10 Histogram for Gage 46

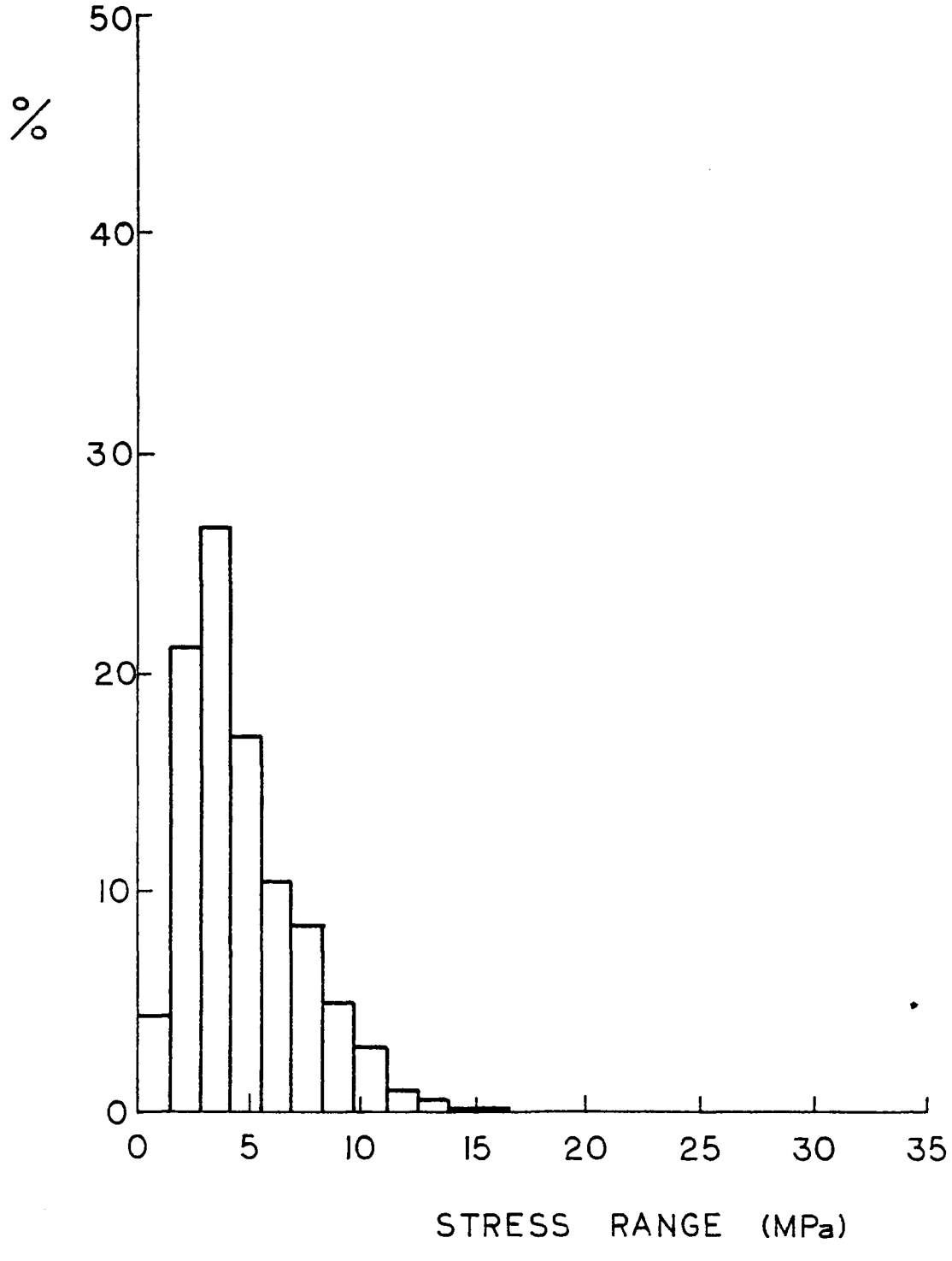

Fig. A.11 Histogram for Gage 50

VITA

The author was born in St. Louis, Missouri on August 7, 1953 to Mr. and Mrs. Joe Inukai.

The author attended Hawthorne Elementary School and Brittany Junior High School in the University City School System. He graduated from University City Senior High School in June of 1971. In May of 1975, he received a Bachelor of Science degree in Civil Engineering from Washington University in St. Louis, Missouri.

The author entered Lehigh University in June of 1975. Since that time, he has been employed as a half-time research assistant in Fritz Engineering Laboratory in the Fatigue and Fracture Division. Most of his work has been on the project "High Cycle Fatigue of Welded Bridge Details". His research in this project has provided the information for this thesis.